

We thank the reviewers for their appreciation for our general approach and for three thoughtful reviews. Below we respond to the issues that are being raised.

## **Response to reviewer 1**

### **Comment**

*The study's applicability to future work is that it can help distinguish between the relative importance of different forcing mechanisms, and highlight where/how we could look for evidence of these processes. There are obviously many simplifications in the model (these are discussed), and these should be borne in mind when assessing the results.*

*For instance, lack of seasonality and no separate boxes for the East and West basins (which each have different run-off, evaporation and ventilation regimes) means that the model could be missing important mechanisms for sapropel formation/preservation.*

### **Response**

We agree, we will add this to the discussion. Seasonality is mostly important as a driving mechanism for the DWF. Including seasonality would require separate intermediate water boxes (increasing complexity), while for the oxygenation deep water only the amount of DWF and mixing with the overlying water mass is truly relevant. Furthermore, we would have to make assumptions regarding the annual variability of the forcing parameters (river outflow and evaporation), which are not well constrained for geological history. We therefore decided to parameterize the seasonal variability, by calculating a yearly averaged DWF flux based on winter temperatures. This allows us to study the fundamental mechanisms of sapropel formation. Perhaps one needs to turn to OGCMs to study the role of seasonal variation. We will add a discussion on the lack of East/West boxes. Also see our comment below regarding lines 233-235.

### **Comment**

*The same goes for potential effects of meltwater pulses (from Atlantic and the EIS).*

### **Response**

We agree that melt water pulses likely affect sapropel formation, but do not consider them to be of first order importance. During many sapropels, melt water pulses did not occur. In future applications of this model where a specific sapropel/interval is studied, drivers such as melt water pulses should of course be included, but this is beyond the scope of this paper. We will add this explanation to section 4.3 (around line 473) in the revised manuscript.

### **Comment**

*I note (lines 233-235) the authors say that 'an arbitrary configuration (and number) of boxes' could be used, so why not use 6 boxes (Boxes 1-3 each for the east and west).*

### **Response**

The aim of a conceptual model is to capture the first order aspects of a process with a minimal setup. As noted by the reviewer, the current setup does this. Doubling the number of boxes would also double the number of forcing parameters and equations, all of which add uncertainty to the model (quantitative reconstruction do not exist for most of these parameters). Moreover, the complexity quickly increases, making it much harder to test and describe the parameter space, and identify key mechanisms. The main purpose of this specific sentence was to point out that the matrix-vector formulation adopted in our paper is applicable equally well to a larger number of boxes. See also our response to a similar question by reviewer 3.

**Comment**

*The authors could also expound on the different DWF mechanisms (line 483), as these are significant for sapropel formation but they are not modelled here.*

**Response**

These two mechanisms are mixing of the water at margins during winter storms, which then cascades to the deep basin, and open ocean convection. This is explained in the Introduction (lines 26-31) and we will refer this in the discussion in the revised manuscript. See also our response to a similar question by reviewer 3.

**Comment**

*Finally, in light of the limitations/caveats, I have an issue with the final 3 lines of the Conclusion - I don't think you can make such a strong conclusion about sapropel formation from this study.*

**Response**

While noting that the start of this sentence makes it clear that this concerns, first and foremost, a suggestion about sapropel formation based on model results, we point out that the conclusion is in line with previous studies (Grant et al., 2016, and references therein) that found that sea surface temperature fluctuations occurred during at least some of the recent sapropels. Here we quantify this effect. With the new formula where oxygen consumption is linearly dependent on oxygen concentration (as suggested by reviewer 3), the role of temperature is more prominent. In the revised manuscript we will add that this conclusion is supported by previous studies.

**Comment**

*However, on a positive note (and I do like this study), the strong agreement between the reference experiments and modern observations (eg deep water fluxes and O<sub>2</sub> concentrations) suggests that the model is nonetheless capturing key processes for sapropel formation. The same goes for the agreement between geological proxy data and the modelled timing and duration of anoxia (and by inference, sapropel formation). I also like the investigation of switching the FW budget, both for the margins and open box, as it hints at what we could expect to see in the sediment record if such a switch occurred.*

**Response**

Thank you, we agree.

**Comment**

*Model duration. The model is run over a full precession cycle, yet it is insolation – which includes an obliquity component – which seems to be the primary driver of long-term African monsoon variability over the Plio-Pleistocene. Modelling studies have demonstrated how obliquity forcing is significant for the African monsoon, and proxy data show the best match with local summer insolation and/or tropical insolation gradients (not all sapropels are associated with precession minima). I assume that going beyond one full precession cycle is beyond the scope of this study, and I appreciate that just to do one full precession cycle is an advance, but some comment on this is needed, especially as the authors state (line 117) that any sine wave could be used.*

**Response**

We are mainly interested in the response of the system to a transient forcing, it is not our aim to reconstruct the exact conditions during specific time intervals. For an individual sapropel, adding an obliquity component would effectively slightly modulate the frequency and amplitude of the forcing. Since the model is not very sensitive to the exact frequency of the forcing, and we already extensively tested the parameter space in terms of amplitude, a simple (20 kyr) sine wave suffices as forcing. We will add a comment to this extent. Also note that since obliquity does not have a

harmonic relation with precession, the modulation would not have the same effect on every sapropel. It likely affects the thickness of a sapropel for example, but the effect may work both ways when comparing different sapropels. Again, this will be added to a new version. Note that line 117 mentions “any temporal variation could be used...”. This implies that the same model code could be applied to different settings/scenarios, or that actual reconstructions (based on sediment cores) or output of other models could be used to force the model rather than just a sine wave.

### **Comment**

*Lags/phasing. The study investigates the phase & duration of sapropels relative to precession as a function of the phase of evaporation, but I think it would be more useful to investigate sapropel timing/duration as a function of the phasing of run-off. The one study they cite re: variable phase of evaporation is for the Miocene, for which we have much less understanding about individual sapropels and their associated E-P, anoxia, etc. Yet many studies have shown links between the timing +/or intensity of palaeo-monsoons and ice-sheet & North Atlantic climate variability, and run-off appears to be the primary driver of sapropel formation.*

### **Response**

Run-off and evaporation are the only transient forcings in the presented model runs, therefore shifting run-off for example 2 kyrs forward in time gives the exact same wave shape as shifting evaporation 2 kyrs backwards in time. The only difference would be that the waveform would be shifted by 4 kyrs. Since we are primarily interested in the transient response rather than the absolute timing, we consider the presented experiments to be sufficient. We will add this description (and note that that the timing of increased river outflow may also vary) to paragraph 3.4.

Minor technical comments

### **Comment**

*Background: A map of the Med with its seas, basins etc may be useful for newcomers to the study of this region. The text mentions the Aegean, Levantine, Adriatic, etc*

### **Response**

Thank you for this suggestion, we will add a map to the revised manuscript.

### **Comment**

*Line 26 & throughout: ‘relatively high latitude’... I think better to refer to the more northerly parts of the basin? I wouldn’t say any of the basin is at a relatively ‘high latitude.*

### **Response**

We do consider the difference in latitude compared to the rest of the basin to be important, as the difference in temperature is a major driver of the circulation in the Mediterranean Sea. We change the sentence to:

“During winter, in the northerly parts of the basin, situated at relatively high latitude, cold and dry winds induce a further density increase, which may lead to the formation of deep water (Schroeder et al., 2012).”

**Comment**

*Line 36: West African summer monsoon (not East). Also some clarification here that the low density surface lid is not due to direct monsoon precipitation over the basin but via run-off*

**Response**

We will change this to “African summer monsoon” (in accordance with Grant et al., 2016, Rohling et al., 2015, etc.). Hennekam et al. (2015) finds that during S1 Nile discharge was likely not predominantly controlled by the West African summer monsoon. We added a clarification that the low density lid is not due to direct monsoon precipitation over the basin.

**Comment**

*Line 51: clarify sapropel mid-point*

**Response**

The average of the top and bottom age, we will add this explanation to in the revised manuscript.

**Comment**

*Line 428: delete ‘thousands’ – the max midpoint phase is <1000. ‘. . . up to hundreds of years’ would be more accurate.*

**Response**

With a higher evaporation variability amplitude, the midpoint phase can shift by more than 1000 years, we will add this remark to the revised manuscript.

**Comments**

*Line 52: perform long runs*

*Line 125: up to 8.8 times*

*Line 145: an efficiency*

*Line 237: Except for the lack of a flux*

*Line 374: reaches*

*Line 458: as long as a sufficiently*

*Line 471: as accurately as possible*

*Line 514 influencing*

*Line 550: deep eater in the open*

*Line 551: by reversing the freshwater budget*

*Line 556: of a hypothetical core*

*Line 566: add Grimm et al 2015*

*Figures 3-6: a-e are not labelled*

*Figures 7-8: font size too small; reorder ‘left/right axis’ in the caption (wrong way around).*

*Figure A1: can’t differentiate between blue & black lines*

**Response**

We acknowledge all these points and will correct them in the revised manuscript.



## Response to reviewer 2

### Comment

*Authors – Only the institution is given. Is there no department or unit?*

### Response

We will add “Department of Earth Sciences” in the revised manuscript.

### Comment

*Introduction: Map, with circulation schematic would be useful to readers who are not familiar with the region.*

### Response

Thank you for this suggestion, we will add a map to the revised manuscript. The lack of this was pointed out by Reviewer 1 also. We do not consider a circulation schematic useful. Figure 1 in the manuscript gives an overview of how the circulation is abstracted in the model, while the articles we refer to (for example Pinardi et al., 2015) give a clear and complete description of the present circulation of the Mediterranean Sea.

### Comment

*Line 64: How are the later two models more advanced?*

### Response

In the revised manuscript we will change this sentence to “...and more recently, using a regional ocean model forced by output from a dedicated global climate model experiment, Mikolajewicz (2011) and Adloff et al. (2011).”

### Comment

*Line 71-77: The description of the box could be improved. Line 76 mentions that the Atlantic box, as well as the rivers are static boxes, yet the Atlantic box has been introduced and defined yet. Figure 1 uses subscripts in many cases, e.g. R1 while the text uses R1. Be consistent through the entire paper.*

### Response

We will correct this in the revised manuscript.

### Comment

*Line 78-87: Again, issues of subscripts or not.*

### Response

We will correct this in the revised manuscript.

### Comment

*The authors mention E-P-R, but P is never defined as precipitation. And given since the box model diagram uses e (lower case), is this then a net evaporation (E-P). Basically, the whole discussion feels a little choppy without it being precisely defined. Additionally, as I was reading this paragraph,*

*I was wondering why no equations. Now, they appear later in the manuscript, in section 2.3. But I'm not sure is the separation of the discussion and the associated equations is the best way to make things clear for the reader. The authors should at least think some more on this, and how best to clearly present their model.*

### Response

We will define P as precipitation and clearly define e/net evaporation. The separation between the description of the model and the presentation of the equations was done on purpose, after careful consideration and based on previous experience with this type of papers. We expect that most

paleoceanographers and biogeologists are not primarily interested in the exact equations, but ought to be able to find in the paper a detailed description of the model. See also our response to a similar question by reviewer 3.

### **Comment**

*Line 110-113: Found these sentences unclear. Please rewrite.*

### **Response**

We will rewrite the sentences in the revised manuscript, along the lines of: “We therefore abstract the circulation to an open surface/intermediate box, a marginal surface/intermediate box and a deep water box, all with constant volumes. While the formation of deep water itself is a seasonal process, we parametrize the seasonal variability by calculating an annually averaged DWF flux. We know that DWF occurs every year during present winters. However, deep water would not form with annual average conditions, we therefore assume perpetual winter conditions.”

### **Comment**

*Line 126: What about outflow/runoff from the Black Sea. What is its magnitude and where is it considered in the model?*

### **Response**

For sapropels during which there is exchange through the Bosphorus strait, the exchange is not constant through time, and also depends on the inflow of Mediterranean water into the Black Sea. Opening or closing of the strait prior to, or during, a sapropel may impact the circulation. When the sill becomes deep enough to allow for a two layer exchange, a large amount of saline water would flow into the Black Sea (following the same principle as at the Gibraltar Strait), thereby causing extra relatively fresh water to flow out into the Mediterranean Sea. During some sapropels, the strait may have been closed. Furthermore, there is very little data regarding the exchange opening and closing of the Bosphorus Strait prior to the most recent opening (approximately 11 ka), perhaps with the exception of the Pontian (which is beyond the scope of this paper).

Consequently, we do not include exchange with the Black Sea. For the cases where there was a steady outflow of fresh water (or an exchange that can be parametrized as such) this could indeed be seen as an extra fresh water source for the margins. We have already tested this effect by varying the river outflow into the margins. We will add this to section 4.3 in the revised manuscript. Please also see our response to a related comment by Reviewer 3.

### **Comment**

*Line 167: Wouldn't a flux approach work better than simple temperature relaxation?*

### **Response**

In a previous version of the model we used a constant flux (of 5 W/m<sup>2</sup>). With a normal circulation this gives similar results, but when the fresh water budget of the margins approaches zero, and the circulation (almost) stops, the results are not realistic. In this situation the margins become almost completely isolated from the rest of the basin, causing a massive temperature drop that doesn't stop until the circulation starts again. In reality this temperature drop would be limited by the atmospheric temperature, hence a relaxation is more realistic. We will add this explanation to section 2.3 in the revised manuscript.

### **Comment**

*Line 239: Subscripts for variables*

### **Response**

We will correct this in the revised manuscript

**Comment**

*Figure 2: Listed as the second figure, but didn't find a reference to it until near the end of the paper. If so, renumber and move to where referred to*

**Response**

We will renumber and move the figure in the revised manuscript.

**Comment**

*One Sentence paragraphs: Appears many times in the paper. They are not proper English and should not be used. In all cases, it should be easy to combine them with surrounding material.*

**Response**

We will combine one sentence paragraphs with the surrounding material in the revised manuscript.

**Comment**

*Line 289: The authors mention that the decrease in vertical density difference causes a decrease in DWF. Yet wouldn't a decrease in the vertical stratification mean that it would be easier to produce deep water formation with the same heat flux?*

**Response**

Indeed, when the deep water has a density that is only slightly above that of the surface water, a given temperature decrease of the surface water would sooner lead to an instable situation and to deep water formation. However, our text at this point refers to a situation in which the overlying water mass (already) has a higher density. Then we expect that a decrease in the density difference will cause a decrease in DWF.

**Comment**

*Line 315: Line stretches into margin*

*Line 321: '...to the DWF one of...'- a word seems to be missing*

**Response**

This should be "...to the DWF of one of...". We will correct this in the revised manuscript.

**Comment**

*Line 322: What is exactly meant by 'within error'*

**Response**

The timing of the sapropel in the model corresponds to the timing found in the cited article within the error margin of the dating of the sediment core. We will add this to the revised manuscript.

**Comment**

*Line 365 (and additionally later in paper): River 1 – Out of river box 1 – i.e. the river flow into the given box, not the flow of a single river*

**Response**

We will correct this in the revised manuscript.

**Comment**

*Line 374: By normal values, do you mean present day?*

**Response**

Yes, we will change this to "present day values" in the revised manuscript.

**Comment**

*Experiments: As I went through the paper, I realized the authors had lots of experiments. This is good in terms of exploring the parameter space and relevant ideas. But hard to keep track of. Please add a table of experiments, listing them, giving them all an easy to follow name, and clearly listing the parameters (so that it is easy to see what is changed in each).*

**Response**

Attached to this response are two tables that give a clear overview of all the presented runs. These we would include in a revised version of the paper.

**Comment**

*Line 396: decrease*

*Line 450: Subscripts*

**Response**

We will correct this in the revised manuscript.

**Comment**

*Line 528: The authors say that exchange through the Bosphorus is out of the scope of paper. Sure, the model can't look at the sea-level changes that lead to that connection. But in terms of impacts, the change is more runoff, which the authors can and do look at with their model. So I don't see this distinction.*

**Response**

To this point we have already responded in the above. See comment to Line 126.

**Comment**

*Line 529: define 'within error*

**Response**

We will correct this in the revised manuscript.

**Comment**

*Line 550: in the open. . .*

*Line 577: . . .system. Without it. . .*

**Response**

We will correct these errors in the revised manuscript.

**Comment**

*Line 578: sufficient sapropels - ??? – word(s) missing*

**Response**

This should be “sufficiently long sapropels”. We will correct this in the revised manuscript.

**Comment**

*Figure A1: I can barely see the difference between the black and blue lines. Use something more distinct. R1 should use a subscript too.*

**Response**

We will correct this in the revised manuscript.

**Comment**

*Table 1: In the descriptions, some fields uses capitals, others don't. Be consistent. Also, be careful with subscripts as elsewhere in the manuscript.*

**Response**

We will correct this in the revised manuscript.

**Comment**

*Figure 3, etc. Panels A, B, C, D, and E are not labelled.*

**Response**

We will correct this in the revised manuscript. See figures 1 and 2 in the attachment for an example.

## Response to reviewer 3

### Comment

*Although I believe that this manuscript is a novel and important study, I have some concerns. Firstly, the authors do not split the Mediterranean into Western and Eastern basins. The straits of Sicily are an important constraint on the circulation of the Mediterranean Sea and the limitation of not including this barrier to deep water circulation is barely discussed. An interesting feature of Sapropels are that they are much more dominant in the Eastern rather than Western basin so I worry about the impact of not separating them.*

### Response

The aim of a conceptual model is to capture the first order aspects of a process with a minimal setup. The current setup does this. Doubling the number of boxes would also double the number of forcing parameters and equations, all of which add uncertainty to the model (quantitative reconstruction do not exist for most of these parameters). Moreover, the complexity quickly increases, making it much harder to test and describe the parameter space, and identify key mechanisms.

This is definitely something we might look into in a future study, but consider it important to first understand the behavior of the a semi-enclosed basin with a gateway before studying what is essentially a second order system. We expect that the effect in the Eastern basin of doing so is similar to the difference between a first order and second order filter: a larger shift of the midpoint (larger group delay), and likely a higher sensitivity. Any resonances in the system are also expected to become more prominent (since the resonant frequencies are now amplified twice). We will discuss this in the revised manuscript.

### Comment

*Secondly I believe that the oxygen model is too simple. The authors use two different constant fluxes to describe oxygen consumption and these are implemented as a step function with a different consumption rate when oxygen is more than and less than 60uM. In models oxygen consumption should be proportional to oxygen concentration with either a rate constant or something like Michaelis Menton/Monod kinetics rather than the step function used here. In addition, Powley et al. (2016) show that oxygen consumption in the Mediterranean varies depending on source of the organic matter reaching the deep ocean, which ideally would be included in the oxygen model. This is important as they show that the Mediterranean has a self-regulating mechanism whereby oxygen consumption decreases when deepwater formation stops due to a lower amounts of DOC reaching the deep waters. More comments concerning this can be found in the detailed comments below.*

### Response

We have now also tried a formulation in which the amount of oxygen consumption is linearly dependent on oxygen concentration, instead of a step function. Although the shape of the dependency between consumption and concentration is different from that implied by Monod kinetics, this new set-up does capture the basic notion of a proportionality to oxygen concentration. The results are very similar when considering everything below 60uM a sapropel, see figures 1 and 2 in the attachment. Fig. 1 is a run with exactly the same forcing as the reference run in the manuscript, and Fig. 2 a run with the exact same forcing as the temperature variability run in the manuscript. Note that in the temperature variability run the minimum in bottom water oxygen is lower and the interval with oxygen below 60uM therefore somewhat longer.

We agree that the feedback related to DOC described by the reviewer is an interesting mechanism to study, however we find that this is beyond the scope of this study. Note that with the new formula oxygen consumption already responds to changes in DWF: as the circulation slows down, less oxygen is supplied to the deep water, causing the oxygen concentration to drop, thereby

reducing oxygen consumption. Furthermore, as a follow-up study we are adapting this water model to a different setting, where we combine it with a nutrient model that includes DOC. While the nutrient model provides further insights, the resulting oxygen concentrations are very similar to the ones found when using both the step function and the linear dependence we use here.

In conclusion, we can adjust the oxygen consumption formula to a linear dependence, this does not significantly affect the main findings. See the attached figures for runs of the first two regimes using this new oxygen consumption formula.

### **Comment**

*In general the written English is good and understandable but I feel that the paper is poorly organised meaning that it is hard to follow what is happening. There are methods in results and results/methods in the discussion. I suggest that the reference simulation and subsequent scenarios are introduced in the methods section with the possibility of a table detailing each simulation. In addition I suggest having separate sections for the oxygen model and building of the water cycle. Finally I suggest that the authors go through the manuscript carefully checking that all acronyms and parameter names are clearly defined somewhere within the paper in addition to using consistent terminology for the boxes and inputs throughout. Can the authors also please crosscheck that all values and figures presented in the text match those in tables and figure numbers in the figure section as there were numerous time where there were inconsistencies.*

### **Response**

We will improve the consistency in the revised manuscript as suggested by the reviewer (also see responses do the detailed comments below). Two tables with the forcing parameters of each presented simulation are attached to this response. These we would include in a revised version.

### **Comment**

*Section 1.2: Please can you include some of the conclusions from the modelling studies*

### **Response**

We will add this to the revised manuscript.

### **Comment**

*Line 71: Please can you explicitly say which areas are in the high latitude marginal basins i.e. does this include the Adriatic and Aegean Seas.*

### **Response**

Yes, this does include the Adriatic and Aegean Seas. We will add this to the revised manuscript.

### **Comment**

*Line 79: Similar to above please can you say the locations where D1 and D2 refer to*

### **Response**

D1 occurs in box 1, and D2 in box 2, so the same locations as these boxes. We will add this explanation to the revised manuscript.

### **Comment**

*Line 128: What about river discharge from Europe? I assume Rhone and Elbe go into the open ocean?*

### **Response**

We assume that the reviewer meant the Rhone and Ebro. In the current model setup, the Gulf of Lyon is considered to be a marginal deep water formation area, thereby included in box 1. The Ebro would indeed flow into the open ocean, although it is relatively unimportant since its present day discharge is only one fifth of that of the Nile.

**Comment**

*Lines 122-134: You report both present day and historic values. What are you using in the your model? It is not clear to me here. You also mention that changes from Europe are not included but then talk about changes from Europe?*

**Response**

We intended to state that Amies et al. (2019) do not include change from Europe. We will replace “this model” by “their study” to explain this more clearly. We do indeed include changes from Europe.

**Comment**

*Section 2.3: Please include somewhere here technical details on running the model. Which method do you use to integrate forward in time, what time step was used, how frequent was the model output?*

**Response**

The equations are integrated numerically simply by the forward Euler method taking appropriately small time steps. We use a time step of 1 year, except when testing the effect of the time step in section 4.2. The curves shown in the figures are built up of the output at every time step. We missed multiplication by  $dt$  in equations 27-29 (only in the manuscript, in the matlab code the equations are correct), e.g., (27) should read  $T(t+1) = T(t) + (G+N+H) \cdot T(t) \cdot W \cdot dt$ . This will be corrected in the revised manuscript.

**Comment**

*Line 145: Here you describe  $c_{13}$  and  $c_{23}$  as an efficiency constant but in Table 1 is described as conductivity between boxes. Please can you either add more description to the text or be consistent in descriptions.*

**Response**

We will change “conductivity” to “efficiency” in the revised manuscript.

**Comment**

*Lines 146-149: I am struggling to understand what is happening here, mostly because the processes such as  $D_2$  were not explained as mentioned above and it all seems rather abstract. What do you mean assuming the DWF in box 2 is the same as box 1?*

**Response**

The deep water formation mechanisms are explained in the introduction, we will refer to the introduction in lines 146-149 in the revised manuscript. We assume that for both of these mechanisms the amount of DWF in a year is linearly dependent on the density difference between the boxes in question.

**Comment**

Please reference the sentence “ $D_2$  does not occur annually”

**Response**

This can be phrased more accurately as “deep convection in the Levantine basin (represented by  $D_2$ ) does not occur every year (Gertman et al, 1994; Pinardi et al., 2015).

**Comment**

*Lines 216-219: The consumption rates for biotic and abiotic oxygen consumption are not the same as in Table 1. I also suggest defining the acronyms for the terms in the text (i.e. biological consumption= OCB). This would also make the terms in equation 22 easier to understand as you wouldn't constantly have to refer to Table 1.*

**Response**

With the new oxygen consumption formula, as suggested by reviewer 3, these parameters are omitted. We agree that defining acronyms in the text would improve readability, and will do so where necessary in the revised manuscript.

**Comment**

*Lines 216-219: Please briefly explain the biotic and abiotic processes. Why is there no biological oxygen consumption below 60uM? Typically oxygen consumption is described using monod kinetics (i.e Vichi et al. (2015), Powley et al. (2016), Testa et al.(2014)) so that it still occurs below 60 uM but is slower. This implemented step function will likely produce the non linearity found in the model.*

**Response**

As explained in the above we have now made oxygen consumption dependent on oxygen concentration, thereby replacing the step function. See also our response to the more general comment. This change yields largely the same results when considering everything below 60uM a sapropel. See the attached figures for preliminary results using this new formula. The step function caused the oxygen concentration to stop decreasing at 60uM, other non-linear behavior is not related to the oxygen consumption formula.

**Comment**

*Line 217-218: Please describe how the oxygen consumption changes with river outflow.*

**Response**

Oxygen consumption increases linearly with river outflow as can be gleaned from Equation (22) in combination with Table 1. In this equation the  $Oc_x$  represent the three types of oxygen consumption.  $Oc_R$  is the coefficient that, upon multiplication with the river discharge, gives the contribution to the rate of oxygen consumption thought related to rivers. This more explicit explanation will be added to the revised manuscript.

**Comment**

*Equation 22: Please define  $R_{tot}$ . It is not mentioned in the text or Table1. I assume it is total river flow which looking at the units for  $OCR$  might be in  $m^3/s$ ? If it is then  $OcR$  would then have to be changed to  $uM/yr$ ? It is also not clear to me why the oxygen consumption is divided by  $dt$  when over 60uM.*

**Response**

$R_{tot}$  is the sum of  $R1$  and  $R2$ , we will correct this in the revised manuscript. With the new oxygen consumption formula the units of the parameters are different, we will carefully check all the units in the revised manuscript.

**Comment**

*Line 225: Initial water temperature? Or water plus air?*

**Response**

The initial temperature of the dynamic boxes. The Atlantic ocean, atmosphere and river boxes are static. The dynamic boxes are boxes 1, 2 and 3, as defined in the methods.

**Comment**

Line 229: What are TA1, TA2 and T0?

**Response**

These are the temperatures of boxes A1, A2, and 0. The abbreviations of the boxes is shown in Fig. 1. We will add this explanation to the revised manuscript.

**Comment**

*Line 231: Where are the winter air temperatures taken from?*

**Response**

These are intended as present day values at the precession maximum. winter SST ranges from  $\sim 10$  °C in the northwest to 15–16 °C in the southeast (Naval Oceanography Command, 1987). We will add this to the revised manuscript.

**Comment**

*Line 233 - 265: Before my next comment I wish to say that I am not used to reading model equations in matrix format, I am used to them as ODEs. However, I found it hard to follow this section and found description of the various matrices were poorly described in some cases, for example what is matrix F or matrix M? In regards to Equation 29, if written in matrix format I would like to see in words what the equation means because as it stands I am not following what is happening and cannot check simple things like units are correct. As a more general comment, I feel it may be better to put this section describing the matrix equations at the beginning of section 2.3 and then explain what how the fluxes and parameters are calculated afterwards.*

**Response**

We acknowledge that the matrix equations are likely difficult to understand for many readers, this is why we have decided to explain all the equations in words before showing them and explaining them mathematically. We will more clearly state that the fluxes (such as  $F_{2,1}$ ) are elements of the matrix F. We think it is more logical to explain the equations of all the fluxes before introducing the matrix calculations, since the fluxes are used in the matrix calculations.

**Comment**

*Section 3: I suggest explaining the different runs in the methods section and potentially having a table describing each simulation and the model setup used.*

**Response**

We consider the runs to be results, since we describe part of the parameter space. We therefore prefer to keep the explanation of the runs in the results. We will add a table describing each run to the results (see tables 1 and 2 in the attachment). We will add a paragraph to the methods where we explain how we tested the parameter space (e.g. identify different regimes in the model).

**Comment**

*Lines 268-276, 332-339 etc: The forcings applied to the runs should be described in the methods section, not here*

**Response**

In the results we describe part of the parameter space. Which part we describe, i.e., what forcing is applied, is in part determined from/inspired by the results of the preceding experiments. It felt as unnatural to make the strict separation suggested by the Reviewer

**Comment**

*Line 320-321: Which value is observational and which is from the model? Please reference the observational data*

**Response**

This sentence will be changed to “The deep water flux at the precession maximum ( $3 \cdot 10^5 \text{ m}^3/\text{s}$ ) is somewhat lower than what is found in observational data ( $1.6 \cdot 10^6 \text{ m}^3/\text{s}$ , Pinardi et al., 2015), although comparable to the DWF one of the Eastern sub basins (Pinardi et al., 2015)”.

**Comment**

*Line 343-345: “we find a sapropel from t=2900 years to 6500 years”. I don’t see this in figure 4E as O2 looks low from around 7000 to 12000 years. In fact to me figure 4E looks remarkable similar to the reference run and I would suggest that you may lookzoom into the mark around 60uM for oxygen concentration. This also means that the conclusion that the addition of atmospheric temperature variability in the model has a large impact on Sapropel formation could be wrong.*

**Response**

The sentence “we find a sapropel from t=2900 years to 6500 years” was erroneously not changed to 7900-11500 after we shifted the timing of the start of the run by 5000 years. We will correct this in the revised manuscript. With the step function formula for oxygen consumption there, the effect of temperature variability is present, but indeed not very prominent in the figures. With the new oxygen formula (where oxygen consumption is linearly dependent on oxygen concentration) the effect of atmospheric temperature variability is more prominent and also more clearly visible.

**Comment**

*Line 365: I can’t see evidence of a positive freshwater budget in Figure 5A.*

**Response**

We currently only show the freshwater budget for the entire basin (which does not change sign in this run), to keep the graphs more readable. We will add the freshwater budget of box 1 separately to the figures in the revised manuscript, figures 1 and 2 in the attachment illustrate this (note that these runs do not have a positive fresh water budget).

**Comment**

*Line 365-366: “the maximum outflow of river 1 is increased from 6.7 .103 to 1.4 .104.” In the reference simulation the maximum outflow of European rivers (I assume R1?) was  $1.2 \times 10^4$ , so I don’t understand: a) where 6.7 comes from and b) how this is different from the reference simulation. I can’t see any noticeable differences in R1 between Fig 3A and Fig 5A either*

**Response**

This was an error, and will be corrected in the revised manuscript. The 6.7 is the minimum outflow of R1. The difference between  $1.2 \times 10^4$  and  $1.4 \times 10^4$  is relatively small, and therefore hard to see in the graph.

**Comment**

*Line 416: What do you mean by irregularities?*

**Response**

The occurrence of multiple local minima. We will add this to the revised manuscript.

**Comment**

*Lines 448-454: This should be in the methods (or maybe results), not opening the discussion.*

**Response**

Point taken. We will move this to the methods in the revised manuscript.

**Comment**

*Lines 456-464: The model timestep is not mentioned in methods so it rather comes out of the blue discussing it here. Also be specific in the writing. Temporal resolution of what? Model outputs or model timestep?*

**Response**

We will mention the model time step in the methods in the revised manuscript, as well as that the model output is generated at every time step. See also in the above (comment to section 2.3).

**Comment**

*Line 470: "Main hypothesis". What is your main hypothesis? This is not stated clearly either here or in the introduction.*

**Response**

With this we refer to the commonly accepted scenario for sapropel formation as it is explained. This is explained in the introduction (lines 34-37), we will explain that we use this as our main hypothesis in the revised manuscript and refer to the introduction when we mention it on line 470.

**Comment**

*Line 483: Please describe the two different mechanisms*

**Response**

This is described on lines 23-31. These two mechanisms are mixing of the water at margins during winter storms, which then sinks to the deep water, and open ocean convection. We will refer to the introduction in the discussion in the revised manuscript.

**Comment**

*Line 509: "A simple threshold analysis will not suffice either". Please explain what you mean be a threshold analysis. Surely the method you are implementing with oxygen is a threshold analysis?*

**Response**

We will rephrase this part to something along the lines of:

"A simple threshold analyses is not ideal either, as the cut-off level can have major impact on both timing and duration, while a clear definition is not readily available. Furthermore, even when the threshold is defined, this method would not be usable for sapropelic marls, which are thought to be the result of the same process, but do not share the same chemical composition. We partly avoid this problem by not considering the midpoint of the sapropel (when assuming a certain oxygen threshold, see subsection 4.5), but also the full wave form (e.g. which intervals could be sapropelic with a slightly different forcing). In the sedimentary record this is generally not possible, since the non-sapropelic intervals do not record all parameters and are often bioturbated. So while our approach can't be related applied to the sedimentary record, it does give insight into factors influence sapropel timing."

**Comment**

*Line 525-527: In the introduction you say Sapropels are caused by African monsoon whereas here you are saying that other mechanisms can cause them. Please clarify in the introduction and go more into depth of different mechanisms and hypotheses for Sapropel formation.*

**Response**

We here mention that sapropel S1 may have been triggered by sea level rise, this does not exclude monsoon intensity variability as the main cause. We will add this to the introduction.

**Comment**

*Line 529: Please can you quantify “within values”, i.e. explicitly compare values in the literature with what you found.*

**Response**

In the model with the new oxygen consumption formula in the run with variable air temperature (Fig. 2 in the attachment) the interval where deep water oxygen is below 60uM lasts from 7.5 to 11.6 kyr (with maximum insolation at 10 kyr), Grant et al. (2016) found that S3 lasted from 80.8-85.8 ka, with an uncertainty of  $2.0 \pm 0.9$  kyr, and the maximum in summer inter-tropical insolation gradient at 82.5 ka. We will change “...within error...” to “...within dating uncertainty...” in the revised manuscript.

**Comment**

*Line 537: What do you mean by strait efficiency?*

**Response**

The magnitude of the density driven flow at the strait for a given density difference, i.e, the coefficient of proportionality between volume transport and density difference. We will add this to the methods.

**Comment**

*Line 539: Please explain what you mean by alternative regimes*

**Response**

Parts of the parameter space where one or more fluxes change direction (as a result of a change in freshwater budget of either part of the basin, or the entire basin), as presented in Figures 5 and 6. We will add a similar description to the revised manuscript.

**Comment**

*Figure 2: Please move to end of paper in line with when it is mentioned in the text.*

**Response**

We will correct this in the revised manuscript.

**Comment**

*Figures 3-6: Please label panels with A,B C, D and E. Please explain for what boxes E-P and E-P-R represent. It would be nice rather than use box 1, 2 etc, you could use marginal , open ocean etc and then it would match up with the text.*

**Response**

We will label panels A, B, C, and D in the revised manuscript, see figures 1 and 2 in the attachment. We prefer to use box 1, 2, etc., to prevent covering a larger part of the graph with the legend. The numbering of the boxes is clearly defined in the methods and Figure 1.

**Comment**

*I also suggest using the same scaling for axes across figures to make comparison between figures easier, for example the scale on the axis for outflow changes in Figure 6A compared to Figure 3A.*

**Response**

Currently the graphs are already very small to accommodate for the axis titles and space between the graphs. We prefer to use as much of the available space as possible. For example, note setting all the axis limits to the same value would imply setting the minimum salinity to approximately 20, which would make the graphs very hard to read.

**Comment**

*Line 122: suggest putting R2 in brackets after box 2 for clarification*

**Response**

We will add R2 in brackets after box 2 in the revised manuscript.

**Comment**

*Line 218: Add additional bracket after 2016*

**Response**

This will be corrected in the revised manuscript

**Comment**

*Line 295+304: Fig 3E rather than Fig. 3D? Line 301: I assume “it “ is oxygen concentration? Be specific*

**Response**

Yes, figure 3E and “it” is oxygen concentration. We will correct this, and revise this part to reflect the results of the new oxygen consumption formula in the revised manuscript.

**Comment**

*Line 273: Suggest putting R2 after Nile outflow for clarification.*

**Response**

We will add R2 after Nile outflow in the revised manuscript.

**Comment**

*Line 354: increase rather than increases*

**Response**

This will be corrected in the revised manuscript

**Comment**

*Line 370: Fig 5E rather than D?*

**Response**

Yes, this will be corrected in the revised manuscript.

**Comment**

*Line 380: “Deep water oxygen largely behaves as the total DWF”. I do not understand this sentence. Please rephrase.*

**Response**

We will rephrase. Deep water oxygen largely correlates with DWF.

**Comment**

*Line 422: “subsection 3.2” The caption for Fig 7 says subsection 3.1*

**Response**

This will be corrected in the revised manuscript.

**Comment**

*Line 456: annual resolution of what? model outputs?*

**Response**

The time step. We will change the sentence to “The time step of one year...” in the revised manuscript.

**Additional Changes**

Besides the points described above, we correct some minor mistake in the equations and moved the atmospheric heat exchange formulas to after the water flux and mixing formulas. A few minor textual errors were corrected as well. Figure 2 of the old version of the manuscript has been removed since it is no longer useful with the new oxygen equation.

#### **Additional references used in our response**

Naval Oceanography Command, 1987. U.S. Navy climatic study of the Mediterranean Sea. Naval Oceanography Command Detachment, Asheville, North Carolina (342 pp.).

# The mechanism of sapropel formation in the Mediterranean Sea: Insight from long duration box-model experiments

Jan Pieter Dirksen<sup>1</sup> and Paul Th. Meijer<sup>1</sup>

<sup>1</sup>Utrecht University, Department of Earth Sciences

**Correspondence:** Jan Pieter Dirksen (j.p.dirksen@uu.nl)

**Abstract.** Periodic bottom water oxygen deficiency in the Mediterranean Sea has led to the deposition of organic rich sediments during geological history, so called sapropels. Although a mechanism linking the formation of these deposits to orbital variability has been derived from the geological record, physics-based proof is limited to snapshot and short time-slice experiments with (Oceanic) General Circulation Models. Specifically, previous modelling studies have investigated atmospheric and 5 oceanographic equilibrium states during orbital extremes (minimum and maximum precession).

In contrast, we use a conceptual box model that allows us to focus on the transient response of the Mediterranean Sea to orbital forcing and investigate the physical processes causing sapropel formation. The model is constrained by present day measurement data, while proxy data offers constraints on the timing of sapropels.

The results demonstrate that it is possible to describe the first order aspects of sapropel formation in a conceptual box model. 10 A systematic model analysis ~~approach~~ provides new insights on features observed in the geological record, such as timing of sapropels, intra-sapropel intensity variations and interruptions. Moreover, given a scenario constrained by geological data, the model allows us to study the transient response of variables and processes that cannot be observed in the geological record. The results suggest that atmospheric temperature variability plays a key role in sapropel formation, and that the timing of the midpoint of a sapropel can shift significantly with a minor change in forcing due to nonlinearities in the system.

## 15 1 Introduction

### 1.1 Background

The response of ocean circulation to changes in atmospheric forcing is an important element of the climate system. Using computer models applied to the geological past we can exploit the sedimentary record of variation in circulation for mechanistic insight. The Mediterranean Sea is of particular interest, as abundant and exceptionally well dated proxy data and present-day 20 measurement data is available and it is a basin that displays processes such as thermohaline circulation and gateway control that play a role on the global scale as well.

Presently, the Mediterranean Sea is an evaporative basin (Romanou et al., 2010) with a small annual mean heat loss to the atmosphere (Song and Yu, 2017). Water from the Atlantic flows in to the Mediterranean Sea at the Strait of Gibraltar and is then subjected to buoyancy loss due to evaporation and cooling ~~-(see Fig. 1 for a map of the Mediterranean Sea)~~. This results

25 in the formation of intermediate water in the Levantine basin which spreads throughout the basin (Hayes et al., 2019; Wu and Haines, 1996).

During winter, in the northerly parts of the basin, situated at relatively high latitude, cold and dry winds induce a further density increase, which may lead to the formation of deep water (Schroeder et al., 2012). Specifically, deep water formation (DWF) occurs over the shallow northern Adriatic Sea (Malanotte-Rizzoli, 1991) and the Aegean Sea (Gertman et al., 2006; 30 Roether et al., 1996) and in the form of open-ocean deep convection in the Gulf of Lion (Marshall and Schott, 1999) and the southern Adriatic Sea (Bensi et al., 2013). Dense water formed in the Adriatic and Aegean Seas, both marginal basins of the Mediterranean Sea, flows out over the seafloor into the deeper parts of the main basin.

The basin's semi-enclosed nature causes the system to be very sensitive to climatic perturbations and the geological record holds an expression of this sensitivity in the form of the regular occurrence of organic rich deposits, known as sapropels 35 (Rossignol-Strick, 1985; Rohling et al., 2015; Hilgen, 1991; Lourens et al., 1996; Cramp and O'Sullivan, 1999). Sapropels are thought to form when freshwater input Nile discharge increases as a response to enhanced EastAfrican summer monsoon activity during precession minima (Rossignol-Strick, 1985; Rohling et al., 2015). The low density fresh water then forms a lid 40 at the surface, stopping or reducing the strength of the overturning circulation. This hypothesis commonly accepted mechanism can be nuanced by noting that the Nile does not enter the basin at a DWF site, but rather close to the location where intermediate water forms. A large part of the DWF involves this intermediate water (Schroeder et al., 2012). Reducing the density of the intermediate water implies a decrease or absence of a (positive) vertical density gradient, also diminishing or stopping the formation of deep water. In contrast, run-off runoff into the marginal basins directly affects the buoyancy at the DWF sites. For deep convection in for example the Levantine basin (which can happen with present day conditions, Gertmann et al., 1994) a decrease in surface water density directly decreases or stops DWF. With decreasing DWF, the supply of oxygen to 45 the deep water diminishes, potentially causing anoxia and the preservation of organic matter in the Eastern Mediterranean Sea. Moreover, nutrient input increases with river outflow as well, thereby affecting primary production, export of organic carbon to the deep water and, consequently, oxygen consumption (Calvert et al., 1992; De Lange and Ten Haven, 1983; Thomson et al., 1999; van Helmond et al., 2015; Weldeab et al., 2003). Sea level rise may also trigger sapropel formation (see Rohling et al., 2015, for sapropel S1), although this does not exclude monsoon intensity variability as the main cause.

50 In this paper we present a simple three box model of the Mediterranean Sea, which includes most mechanisms elements commonly invoked to explain sapropel formation as described above. With the model we study which processes determine when and why sapropels form the way they do. Our aim is to gain a new perspective on the timing of the sapropel, relative to the forcing, as a significant part of the late Neogene geological time scale depends on this relation (Hilgen et al., 1995; Krijgsman et al., 1999) and views on the timing of the mid-point midpoint (the average of the top and bottom age) are contested in more 55 recent publications (Channell et al., 2010; Westerhold et al., 2012, 2015). A low complexity model allow us to do perform long runs and explore the parameter space to a much greater extent than high complexity models. Long runs are necessary to study the transient response of the system over a full precession cycle.

As described in modelling studies (such as Marzocchi et al., 2015) as well as in observational studies (for example Herbert et al., 2015), surface air temperatures have also been found to vary over a precession cycle, where precession minima are

60 estimated to have been 1-3 °C warmer (annual average) than precession maxima. Since heat loss depends on the temperature difference between the water surface and atmosphere, this is another factor that decreases buoyancy loss during precession minima. We will examine the relative importance of this effect by running the model both with, and without atmospheric temperature variability.

## 1.2 Previous modelling studies

65 Just like the Last Glacial Maximum, the time of sapropel formation has been recognized early on in the application of OGCMs to Mediterranean circulation, as a configuration that makes for an interesting contrast to the present-day state (Bigg, 1994; Myers et al., 1998; Myers and Rohling, 2000; Myers, 2002; Meijer and Tuenter, 2007; Meijer and Dijkstra, 2009); and more recently, using a ~~more advanced model~~ regional ocean model forced by output from a dedicated global climate model experiment, (Mikolajewicz, 2011; Adloff et al., 2011). Several studies have explored the coupling of circulation models to models of the 70 biogeochemical cycling, first offline and then in truly combined fashion (Stratford et al., 2000; Bianchi et al., 2006; Grimm et al., 2015). All these studies have in common that they are limited to time spans much shorter than the precessional cycle. The only previous box models related to the sapropel problem are those by Matthiesen and Haines (2003) and Amies et al. (2019), but these models lacks a representation of the deep waters of the basin.

75 The previous offer support for the basic idea that freshening of the surface waters leads to reduction of the overturning circulation. The studies suggest that it is important to consider the full fresh water budget and that runoff may have varied significantly on orbital time scales (Bigg, 1994; Amies et al., 2019). Finally, nutrient supply is found be a significant factor in the formation of sapropels (Stratford et al., 2000; Bianchi et al., 2006).

## 2 Methods

### 2.1 Model set-up

80 The Mediterranean Sea is represented by three boxes in our model: the high latitude marginal basins (intermediate and surface water, box 1, representing the Adriatic and Aegean Seas and the Gulf of Lion), the open Mediterranean (surface and intermediate water, box 2) and the deep water (box 3) (see Fig. 2). Box 1 and 2 have fluvial input (sourced from boxes ~~R1 and R2~~ R1 and R2, see Fig. 2) and exchange with the atmosphere (represented by boxes ~~A1 and A2~~ A1 and A2, see Fig. 2). The surface forcing is further explained in subsection 2.2. Each box has its own temperature and salinity. Boxes 1 through 3 are dynamic: 85 the temperature, salinity and density is calculated during each time step, based on the incoming and outgoing salt and heat. The Atlantic, both rivers and both parts of the atmosphere can be seen as static boxes: their salinity, temperature and density are constant.

90 Circulation is modelled by including downward, vertical fluxes, of which the magnitude depends on the density difference between the surface/intermediate layer and the deep water (~~D1 and D2 in D1 in box 1 and D2 in box 2 in~~ Fig. 2). This DWF is driven by buoyancy loss, due to ~~evaporation (e1 and e2) net evaporation (E-P, where E is the evaporation and P precipitation, e1~~

and  $e_2$  in Fig. 2) and heat exchange with the atmosphere, which is modelled as a relaxation (i.e. the surface water temperature relaxes to the temperature of the associated atmosphere box, fluxes  $H$  and  $I_2$ ,  $I_1$  and  $I_2$  in Fig. 2). Note that the DWF in box 1 captures the behaviour of the marginal basins of the Eastern Mediterranean sea, but is also an approximation of the open ocean convection in the Gulf of Lyon (see subsection 1.1). In the typical situation that the Mediterranean surface/intermediate water at the Strait of Gibraltar is more dense ~~then than~~ the Atlantic water and E-P-R ~~is positive (net evaporation)~~ ~~(the fresh water budget, where R is the total runoff)~~ ~~is positive~~, it is the outflow to the Atlantic ( $Q_o$  in Fig. 2) that depends on the density difference between the adjacent water masses. The inflow into the Mediterranean Sea is then the sum of the outflow to the Atlantic and the ~~net evaporation (E-P-R)~~ ~~fresh water budget~~. The equations used in the model are further explained in subsection 2.3.

100 In addition to the water fluxes, diffusive mixing is also included in the model. In contrast to the water fluxes, no net water transport occurs as a result of the mixing. Rather, properties are exchanged between adjacent boxes. The amount of horizontal mixing (between the upper boxes) is constant, while the vertical mixing is a function of the density difference between the boxes in question.

105 A first order approximation of deep water oxygen concentration is included in the model to get a better understanding of when oxygen deficiency occurs. The oxygen concentration of the upper boxes is assumed to be in equilibrium with the atmosphere and is therefore constant. The oxygen concentration of the deep water (box 3) depends on the deep water fluxes, mixing and oxygen consumption. Oxygen consumption ~~depends on is scaled with~~ river outflow, as a first order approximation of the nutrient input, and oxygen concentration. ~~When the oxygen concentration drops below a threshold level, aerobic respiration is assumed to stop, reducing the oxygen consumption to a background level.~~ The use of constant volume for the boxes implies 110 (i) that we take there to always be a distinction between surface/intermediate and deep cell, and (ii) that the upper cell always extends to the same depth. The upper cell appears to be set up by the exchange with the ocean (see Meijer and Dijkstra, 2009, for the Mediterranean Sea and Finnigan et al., 2001, for a generic buoyancy-driven marginal sea) and is likely a persistent feature of Mediterranean circulation as long as there is an exchange flow. Moreover, starting from a state that does have DWF and a separate deep cell, OGCM experiments of reduced net evaporation show a halting of deep circulation while keeping the 115 upper cell more or less in place (Meijer and Dijkstra, 2009).

120 In the present-day Mediterranean Sea DWF is the last step in a chain of processes (See ~~see~~ the introduction). Our model does not include the intra-annual variability, and the basin geometry is only represented in abstract form. However, in the sense that the model does capture both the effect of salinity increase and temperature decrease on upper-water density it is expected to form a fair representation, qualitatively speaking, of the essence of the overturning circulation. To which extent this is true will have to follow from more advanced models. Note that the model of Matthiesen and Haines (2003) also neglects the seasonal cycle. During winter, convection occurs (Schroeder et al., 2012) and the depth of the intermediate water is relatively stable. We ~~can therefore reduce the conceptual model therefore abstract the circulation~~ to an open surface/intermediate box, a marginal surface/intermediate box and a deep water box, all with constant volumes. While the formation of deep water ~~it self itself~~ is a seasonal process, we parametrize the seasonal variability by calculating an annually averaged DWF flux. ~~To do so, perpetual winter conditions have to be assumed, as~~ ~~We know that DWF occurs every year during present winters. However,~~ deep water

would not form with annual average conditions, while we know that DWF occurs during present winters and therefore we assume perpetual winter conditions.

## 2.2 Surface forcing

The transient response of circulation and water properties to precession induced climate change is modelled by altering the evaporation and river outflow for each box at every time-step. The analyses presented in this paper all use sine-waves to force the model, but any temporal variation could be used, such as that of the insolation curve. To be precise, the model forcing used in this paper is derived from a normalized sine-wave with a 20 kyr period, to reflect climatic precession. The amplitude and offset is then altered for evaporation and fluvial discharge in boxes 1 and 2. The phase of evaporation relative to the precession forcing is uncertain (see subsection 3.4) and is therefore varied between runs. The phase of the river discharge is kept at 0 degrees.

The fluvial discharge in box 2 ( $R_2$ ) is interpreted as the Nile outflow and other run-off runoff from Africa. Prior to the construction of the Aswan High Dam in 1964, average Nile discharge was  $2.7 \cdot 10^3 \text{ m}^3/\text{s}$  (Rohling et al., 2015). Present day runoff from Africa is approximately  $1.4 \cdot 10^3 \text{ m}^3/\text{s}$  (Struglia et al., 2004). A recent modelling study (Amies et al., 2019) suggests that peak runoff from Africa may have been up to 8.8 times larger than present during sapropel S5, note that this model. That their study does not consider changes in outflow from Europe.

Fluvial discharge into the high latitude marginal basins of the Mediterranean Sea ( $R_1$  in the model) is presently approximately  $6.7 \cdot 10^3 \text{ m}^3/\text{s}$  (Struglia et al., 2004). Increased runoff from Europe into the eastern Mediterranean has been proposed as a possible source for extra fresh water during precession minima (Rossignol-Strick, 1985; Rohling et al., 2002; Scrivner et al., 2004)

The current net evaporation (E-P) is approximately  $0.9 \text{ m/yr}$  (Romanou et al., 2010). During sapropel times, net evaporation is hypothesized to have decreased (Rohling, 1994), although this has not been quantified. We therefore test a broad range of net evaporation, from 0.2 to  $2 \text{ m/yr}$  to accommodate for these uncertainties.

## 2.3 Model equations and parameters

Here we first discuss the flux equations resulting from the model set-up and assumptions described above, followed by the equations used to integrate all flux-equations into a fully functioning model. All parameters are given in Table 1.

We use a matrix vector representation to calculate the temperatures, salinities, densities, oxygen concentration of the next time step. The (water and heat) flux magnitudes and mixing intensities define the elements of the matrices used for these calculations. This same matrix-vector representation could be used for an arbitrary configuration (and number) of boxes, to represent different oceanographic settings. Observational and modelling studies (Herrmann et al., 2008; Schroeder et al., 2012) have shown that during colder winters, more deep water is formed. Hence, it makes sense that the magnitude of the vertical, downward fluxes ( $D_1$  and  $D_2$ , see equations Eqs. 2 and 3) depends on oceanographic (and thereby indirectly also atmospheric) conditions. The most simple way of implementing this behaviour on a yearly resolution, is to assume a linear relationship between the density difference and flux magnitude (similar to Matthiesen and Haines (2003)

)(similar to Matthiesen and Haines, 2003). When the density of the overlying water mass is smaller than that of the deep water, the water column is stratified and no vertical flux exists. To clip negative components of a flux to 0, we use the form  $F_{j,i} = \max(0, a)$ , where  $a$  is the flux in question. We therefore define the following mathematical operator:

$$\max(a, b) = \begin{cases} a & \text{for } b \leq a \\ b & \text{for } b > a \end{cases} \quad (1)$$

The proportionality of DWF to surface to deep water density difference is determined by a~~an~~ efficiency constant,  $c_{13}$  and  $c_{23}$  for  $D_1$  and  $D_2$  respectively. The magnitude of these constants is chosen in such a way that a realistic deep water flux occurs at a present-day density difference. In the current circulation ~~D<sub>2</sub> deep convection in the Levantine basin (represented by D2)~~ does not occur ~~annually, every year~~ (Gertman et al., 1994; Pinardi et al., 2015), making it difficult to determine  $c_{23}$  empirically. By assuming that the DWF process in box 2 is the same as in box 1 ~~(i.e. linearly dependent on the vertical density difference)~~,  $c_{23}$  can be taken as 4 times larger than  $c_{13}$ , proportional to the difference in surface area of boxes 1 and 2. We therefore define the DWF fluxes in ~~equations Eqs.~~ 2 and 3, ~~where  $\rho_1$ ,  $\rho_2$  and  $\rho_3$  are the densities of boxes 1 to 3 respectively.~~

170  $D_1 = \max(0, c_{13} \cdot (\rho_1 - \rho_3)) \quad (2)$

$D_2 = \max(0, c_{23} \cdot (\rho_2 - \rho_3)) \quad (3)$

At the Strait of Gibraltar, the exchange has two components from which the in- and outflow is calculated (see equations below): a density driven flux  $Q_o$  (Eq. 4) and a compensating flux  $Q_i$  (Eq. 5). The magnitude of  $Q_o$  has a square-root relation to the horizontal density difference at the strait ~~(where  $\rho_0$  is the density of the Atlantic ocean)~~, in accordance with ~~(Bryden and Kinder, 1991)~~ [Bryden and Kinder \(1991\)](#). Theoretically, this flux should be able to change direction, when the density difference changes sign. We therefore multiply the square-root of the absolute value of the density difference with the sign of the density difference. Note that the direction of the fluxes (i.e. whether it goes in or out of the Mediterranean Sea) is determined in ~~equations Eqs.~~ 11 and 10. The ~~conductivity parameter strait efficiency~~  $c_{20}$  ~~(the coefficient of proportionality between volume transport and density difference)~~ is again calibrated on present-day conditions (Schroeder et al., 2012; Jordà et al., 2017; Hayes et al., 2019). The compensating flux  $Q_i$  can then be calculated as the difference of  $Q_o$  and the total freshwater budget of the Mediterranean Sea, to allow for conservation of volume.

$$Q_o = \begin{cases} -c_{20} \cdot \sqrt{|\rho_2 - \rho_0|} & \text{for } \rho_2 \leq \rho_0 \\ c_{20} \cdot \sqrt{|\rho_2 - \rho_0|} & \text{for } \rho_2 > \rho_0 \end{cases} \quad (4)$$

185  $Q_i = Q_o - R_1 - R_2 + e_1 + e_2 \quad (5)$

Heat exchange with the atmosphere depends on the temperature gradient with the surface water, thereby relaxing the temperature of the surface box to that of the atmosphere, similar to Ashkenazy et al. (2012). The heat exchange therefore is calculated by multiplying the temperature difference between the atmosphere and water box by a relaxation parameter. This relaxation parameter depends on the density of the water. In the model we rewrite this to an equivalent volume flux,  $H_1$  and  $H_2$  (in  $m^3/s$ ), so that they can be treated as volume fluxes in the calculation of  $dT/dt$ . The constants that relate the temperature and temperature gradient to a heat flux ( $c_{1A1}$  and  $c_{2A2}$  in equations 20 and 21) are chosen so that at present day temperatures, a heat flux of approximately  $5 \text{ W/m}^2$  occurs, in accordance with Song and Yu (2017) and Schroeder et al. (2012).  $c_p$  is the specific heat of water.

$$H_{1,A1} = \frac{c_{1A1}}{c_p \cdot \rho_1}$$

$$H_{2,A2} = \frac{c_{2A2}}{c_p \cdot \rho_1}$$

The equations above describe all fluxes driven by gradients. By combining these fluxes with the surface forcing, we can derive the other fluxes by assuming constant box volume. The next set of equations (Eq. 6-16) define elements of a matrix  $\mathbf{F}$ , representing all water fluxes.

$$200 \quad F_{1,A1} = e_1 \quad (6)$$

$$F_{2,A2} = e_2 \quad (7)$$

$$F_{R1,1} = R_1 \quad (8)$$

$$205 \quad F_{R2,2} = R_2 \quad (9)$$

$$F_{2,0} = \max(0, -Q_i) + \max(0, Q_o) \quad (10)$$

$$210 \quad F_{0,2} = \max(0, Q_i) + \max(0, -Q_o) \quad (11)$$

$$F_{2,1} = \max(0, F_{13} - F_{R11} + F_{1A1}) \quad (12)$$

$$F_{1,2} = \max(0, -F_{13} + F_{R11} - F_{1A1}) \quad (13)$$

215

$$F_{1,3} = D_1 \quad (14)$$

$$F_{2,3} = D_2 \quad (15)$$

$$220 \quad F_{3,2} = D_1 + D_2 \quad (16)$$

Mixing has a major impact on oceanic circulation, and must therefore be included in the model. Unlike the water fluxes described above, mixing does not cause a net water transport between boxes, but rather an exchange of properties (salt, heat and oxygen). In the model, we distinguish between horizontal and vertical mixing. Horizontal mixing, between boxes 1 and 2, depends on a fixed length scale over which mixing occurs and diffusivity (see Eq. 17). Vertical mixing (see [equations Eq. 18](#) and 19) depends on the density difference between the boxes in question, where a larger density gradient causes more mixing.

225 [d<sub>1</sub>, d<sub>2</sub> and d<sub>3</sub> in Eq 18 and 19 are the depths of boxes 1, 2 and 3 respectively and A<sub>1</sub> and A<sub>2</sub> the surface areas of boxes 1 and 2.](#) Thereby the diffusivity of vertical mixing effectively depends on the density difference. When the water column is stratified, mixing does not stop completely, but rather decreases to a background level, representing the internal waves and other disturbances. In the model this is included by clipping the vertical mixing to a fixed level ( $k_{bg}$ ) when the density gradient 230 becomes very small or negative. [Equations 17-19 define elements of a matrix M.](#)

$$m_{1,2} = k_{12} \cdot L \quad (17)$$

$$m_{1,3} = \max(k_{bg}, (\rho_1 - \rho_3) \cdot k_{str} + k_{bg}) \cdot \frac{2 \cdot A_1}{\underline{Wc_1} \frac{d_1 + d_3}{d_1 + d_3}} \quad (18)$$

235  $m_{2,3} = \max(k_{bg}, (\rho_2 - \rho_3) \cdot k_{str} + k_{bg}) \cdot \frac{2 \cdot A_2}{\underline{Wc_2} \frac{d_2 + d_3}{d_2 + d_3}} \quad (19)$

[In our model, heat exchange with the atmosphere is represented by a relaxation to a prescribed air temperature \(e.g. Ashkenazy et al., 2012\).](#) When one uses a prescribed heat flux instead, in general similar results are obtained. However, when the fresh water budget of the margins approaches zero and the circulation (almost) stops, the results are not realistic. In this situation the margins

240 become almost completely isolated from the rest of the basin, causing a massive temperature drop that does not stop until the circulation starts again. In reality this temperature drop would be limited by the atmospheric temperature, something the relaxation representation does capture.

245 We thus multiply the temperature difference between the atmosphere and the water by a relaxation parameter  $c_A$  in  $W/(m^2 \cdot K)$ . The value of this parameter is chosen such that at present day temperatures, a heat loss to the atmosphere of approximately  $5 \text{ W/m}^2$  occurs, in accordance with Song and Yu (2017) and Schroeder et al. (2012). In the matrix-vector representation the two relaxation boundary conditions correspond, upon the necessary conversion, to two elements of a matrix  $\mathbf{H}$ .

250 In a previous version of the model we used a constant flux (of  $5 \text{ W/m}^2$ ). With a present-day circulation this gives similar results, however, when the fresh water budget of the margins approaches zero, and the circulation (almost) stops, the results are not realistic. In this situation the margins become almost completely isolated from the rest of the basin, causing a massive temperature drop that doesn't stop until the circulation starts again. In reality this temperature drop would be limited by the atmospheric temperature, hence we use a relaxation.

$$H_{1,A1} = \frac{c_A \cdot A_1}{c_p \cdot \rho_1} \quad (20)$$

$$H_{2,A2} = \frac{c_A \cdot A_2}{c_p \cdot \rho_2} \quad (21)$$

Oxygen is supplied to the deep water from the surface by fluxes  $D_1$  and  $D_2$  (equations 2 and 3) as well as through mixing with boxes 1 and 2 ( $m_{1,3}$  and  $m_{2,3}$ , equations 18 and 19). The oxygen concentration in boxes 1 and 2 is assumed to be in equilibrium with the atmosphere and therefore constant. For the deep water, ~~three oxygen consumption regimes are defined: when oxygen consumption depends on the oxygen concentration is above  $60 \mu M$ , the deep and benthic fauna is assumed to be stable and biological plus abiotic oxygen consumption is set to  $0.4 \mu M$  in total per year (corresponding to  $1 \cdot 10^{12} \text{ mol/yr}$ , following Powley et al. (2016) of the deep water and river outflow. River outflow also affects oxygen consumption in this regime. With a deep water oxygen concentration between  $60$  and  $0 \mu M$ , only abiotic oxygen consumption occurs, which is set to  $0.2 \mu M$  per year~~ increases oxygen consumption, while lower oxygen concentrations decrease oxygen consumption. When the deep water is completely anoxic, oxygen consumption stops as well. Other processes affecting sapropel formation, such as nutrient dynamics and increased productivity due to the development of a deep chlorophyll maximum (Rohling et al., 2015; De Lange et al., 2008; Kemp et al., 1999; Rohling and Gieskes, 1989; Slomp et al., 2002; Van Santvoort et al., 1996; Santvoort et al., 1997) are not explicitly included in the model, but are to some extent parametrized by the ~~dependency dependence~~ of oxygen consumption on the total river outflow (see equation 22). The total river outflow ( $R_{tot}$ ) is defined as  $R_1 + R_2$ . Oxygen consumption increases linearly with river outflow as can be gleaned from Eq. 22 ~~in combination with Table 1~~.  $O_{CR}$  is the coefficient that, upon multiplication with the river discharge, gives the contribution to the amount of oxygen consumption related to river discharge. The constant  $O_{CO}$  scales oxygen use with the oxygen concentration.

270  $O_{consumption} = \max(0, (O_{CO} + R_{tot} \cdot O_{CR}) \cdot O/dt)$  (22)

The model parameters (excluding surface forcing) used in all runs are given in Table 1. Initial temperatures are set to 16 °C and salinities to 37 for all dynamic boxes; ~~they~~. They have no effect on the outcome of the model runs after spin-up. With the strait efficiency used in this paper, the model has a typical equilibrium time of less than 1000 years, while a spin-up of 20 kyr is removed from the output. ~~As the~~ The temperature in boxes 1 and 2 relaxes to both the Atlantic temperature and the 275 air temperatures, ~~TA1, TA2 and T0~~  $T_0, T_{A1}, T_{A2}$  respectively.  $T_0, T_{A1}, T_{A2}$  therefore effectively set the temperature range of ~~boxes 1, 2 and 3~~. The dynamic boxes. The winter air temperatures are within the range given by the Naval Oceanography Command (1987): 10°C in the northwest to 15 – 16°C in the southeast. The river inflow also affects temperature, but has a much smaller impact due to the relatively small amount of water (2 orders of magnitude smaller than the Atlantic exchange). The air temperatures are chosen as winter values, since average air temperatures do not result in a realistic atmospheric heat 280 loss and DWF. The temperature of the river water does not have a large influence on the model outcome.

The ~~numerical integration of the model is best thought of as a matrix-vector representation. This same set-up could be used for an arbitrary configuration (and number) of boxes, to represent different oceanographic settings. The~~ volumes of the boxes are calculated from the depth and surface area for all dynamic boxes, where  $V, A$  and  $d$  are all vectors with three elements:

$$V = A \cdot d \quad (23)$$

285 Except for the lack of a flux from box 3 to box 1, water can flow between all boxes in both directions. In the model, three types of fluxes exist: predefined fluxes, density driven fluxes and balancing fluxes. The predefined fluxes are used to force the model: evaporation and river discharge. The density driven fluxes are the DWF (unidirectional) and, depending on the sign of the density difference, Atlantic inflow or Mediterranean outflow. All other fluxes are of such magnitude that volume is preserved. During each ~~time-step~~ time step in the model, the salinity, temperature and density for the next ~~time-step~~ time step 290 are calculated from the fluxes and mixing. In the model script, these equations are only defined for dynamic boxes, increasing the model efficiency significantly. Below the equations are given in matrix form. The volumes of static boxes are infinite, as their temperature and salinity do not change, regardless of in- and outgoing fluxes. Note that the atmosphere boxes are the last two boxes in matrix  $\mathbf{F}$  (boxes  $n$  and  $n - 1$ ).

The matrix  $\mathbf{G}$  describes the water fluxes for the calculation of the new temperature, where  $\mathbf{I}$  is the identity matrix and  $\mathbf{l}$  the 295 unit vector.

$$\mathbf{G} = \mathbf{F} + \mathbf{I} \cdot \sum_j \mathbf{F}_{ij} \cdot \mathbf{l}_i \quad (24)$$

The matrix  $\mathbf{P}$  describes the water fluxes for the calculation of the new salinity, where  $\mathbf{J}$  is a matrix of ones. The only difference with  $\mathbf{G}$  being that evaporation is excluded (since evaporated water does not contain salt).

$$\mathbf{P} = \mathbf{F} + \mathbf{I} \cdot (\mathbf{J}_{n,1} - (\mathbf{l}_n + \mathbf{l}_{n-1})) \cdot \sum_j \mathbf{F}_{ij} \cdot \mathbf{l}_i \quad (25)$$

$$\mathbf{N} = \mathbf{M} + \mathbf{I} \cdot \sum_j \mathbf{M}_{ij} \cdot \mathbf{l}_i \quad (26)$$

$\mathbf{W}$  is a vector so that  $W_i = \frac{1}{V_i}$ .

Similar to  $\mathbf{F}$ , the heat fluxes (equations 20 and 21) are placed in  $\mathbf{H}$ , which is of the same size as  $\mathbf{F}$  and where all undefined elements are zero. We use a time step,  $dt$ , of 1 year, unless noted otherwise. Then the change in temperature for each time-step equals: time step equals:

$$\mathbf{T}(t+1) = \mathbf{T}(t) + (\mathbf{G} + \mathbf{N} + \mathbf{H}) \cdot \mathbf{T}(t) \cdot \mathbf{W} \cdot dt \quad (27)$$

and for salinity:

$$\mathbf{S}(t+1) = \mathbf{S}(t) + (\mathbf{P} + \mathbf{N}) \cdot \mathbf{S}(t) \cdot \mathbf{W} \cdot dt \quad (28)$$

The density for the next time step is calculated from the temperature and salinity using the EOS80 formula (on Oceanographic Tables, 1986). Note that vectors  $\mathbf{V}, \mathbf{S}, \mathbf{T}$  and  $\rho$  include both static and dynamic boxes.

The deep water oxygen concentration of the next time step is similarly:

$$\mathbf{O}(t+1) = \max(0, \mathbf{O}(t) + (\mathbf{F} \mathbf{P} + \mathbf{M} - \mathbf{N} - \mathbf{O}_{consumption}) \cdot \mathbf{O}(t) \cdot \mathbf{W} \cdot dt) \quad (29)$$

Note that the oxygen concentration is only calculated for the deep water (making  $\mathbf{O}$  and  $\mathbf{O}_{consumption}$  effectively scalars) and that the surface water boxes have a constant oxygen concentration.

315 The equations are integrated numerically by the forward Euler method taking appropriately small time steps. The figures shown below are built up of the output at every time step.

## 2.4 Statistical analysis

One of the results of the model is that slight variations of forcing parameters can cause significantly different sapropel duration and timing. We therefore introduce a statistical test to determine the magnitude thereof, given the uncertainty of each of the 320 forcing variables. With eleven forcing parameters (the phase of evaporation and minima and maxima of  $R_1, R_2, T_{A1}, T_{A2}$  and evaporation) it is not feasible to calculate all permutations at a meaningful resolution. We therefore randomly pick and run 200 permutations (fewer permutations would produce unreliable results), given the uncertainty of each parameter, and calculate the  $1\sigma$  and minimum and maximum values of the resulting oxygen concentrations per time step (see Fig. A1 for an example). During testing, we can thereby visualize much more of the parameter space than when doing individual runs.

### 3.1 Reference experiment

In the reference experiment the sine functions for the forcing are calibrated such that the precession maximum corresponds to present-day values—given that the orbital configuration is close to a precession maximum today. The curves are shown in Fig. 3A. All runs use a spin up of a full precession cycle, which is excluded from the figures and analyses; model run time T 330 (horizontal axes) is set to 0 at the end of the spin up. All figures show an entire precession cycle, with the precession maxima falling at T=0 and T=20 kyr. The precession minimum sits at T=10 kyr.

Nile outflow ( $R_2$ ) increases from  $5 \cdot 10^3$  to  $3 \cdot 10^4 \text{ m}^3/\text{s}$ , while river outflow from Europe only increases from  $5 \cdot 10^3$  to  $1.2 \cdot 10^4 \text{ m}^3/\text{s}$  and evaporation decreases from 0.9 to 0.75  $\text{m}/\text{yr}$ . While quantitative reconstructions of fluvial discharge and evaporation during sapropel formation are not available, these minimum and maximum values are in agreement with Marzocchi 335 et al. (2015). All other parameters, found in Table 1, do not vary with time. [Table 2 shows the forcing parameters that are the same for all presented runs and Table 3 gives the forcing parameters that are changed between runs.](#)

From Time=0 towards the precession minimum, the river outflow increases and, as a result, salinities decrease, as shown in Fig. 3B. After the precession minimum river outflow decreases again and salinities increase. The differences in salinity between the boxes decreases towards the precession minimum, and increases again after the precession minimum. The amplitude of the 340 salinity variability is much smaller in the open Mediterranean box (Box 2), as it is connected to the Atlantic (Box 0), which has a constant salinity in this run. Deep water salinity (Box 3) lags the salinity of the upper boxes (this will be interpreted after describing the other graphs). As a result of this behaviour, the salinity of the marginal box (Box 1) briefly drops below the deep water salinity just prior to the precession minimum.

The temperatures, shown in Fig. 3C, do not change drastically, except for a decrease in temperature at the margins in the 345 interval surrounding the precession minimum (we will come back to this below).

As temperature does not change much, density variability (Fig. 3D) is largely determined by changes in salinity. The dip in marginal temperature has an opposite effect on density compared to the salinity fluctuation, consequently the decrease in surface to deep density gradient is relatively small, and the marginal density does not drop below the deep water density.

Nevertheless, the decrease in the vertical density difference causes a decrease in DWF ( $D_1$  in  $D_1$  Fig. 3E, also see [Eq. 350 equation 2](#)). DWF in the open Mediterranean box ( $D_2$ ) does not occur in this run, since the density in the upper open Mediterranean box never exceeds the density of the deep water box. The cause of the previously mentioned dip in marginal temperature, lies in the reduction of DWF which in turn decreases the inflow of water from the open Mediterranean to the margins ([Eq. equation 12](#)). The decrease in supply of relatively warm water to the margins causes the water temperature of the margins to approach the much lower atmospheric temperature.

355 The outflow to the Atlantic ( $Q_0$ , in Fig. 3D) depends on the density difference between the open Mediterranean and the Atlantic. Since the properties of the Atlantic water are kept constant in all presented model runs, the outflow only depends on the density of the open Mediterranean box. As expected then, the decrease in density of the open Mediterranean water in the interval surrounding the precession minimum causes a slight decrease in outflow to the Atlantic.

The deep water oxygen concentration (Fig. 3D) depends on 4(i) oxygen consumption, and 2(ii) DWF and vertical mixing.

360 When the oxygen concentration is above  $60 \mu\text{M}$ , it The deep water oxygen concentration largely follows the same trend as DWF. Below  $60 \mu\text{M}$  oxygen consumption is much lower, causing it to not drop any further (see Eq. 22). From roughly 9-20 kyr the deep water oxygen has a phase lead relative to DWF. Note that DWF does not have to stop completely to cause a decrease in the oxygen concentration; when the oxygen consumption combined with the out-flowing oxygen exceeds the supply of new oxygen, the deep water oxygen concentration decreases.

365 As we have seen in the description of Fig. 3D, the salinity decrease occurs in both the margins (where the deep water forms in this run) and the open Mediterranean (where the water that flows to the margins originates from). The deep water salinity depends on DWF and mixing with the overlying boxes. Consequently, the deep water salinity always lags the salinity of the upper boxes. The amount of lag between the deep and the surface boxes depends on the water and property exchange with the deep box and is therefore not constant throughout the run. At the precession minimum, the lag is in the order 200 years. As the increase in river outflow towards the precession minimum reduces DWF and mixing, the lag between deep and surface/intermediate water salinity also increases (too subtle to see in the graphs). As a result, there is a brief period, starting 1800 years before the precession minimum and ending 440 years after the precession minimum for the margins and 580 years for the open Mediterranean, where deep water salinity is higher than surface/intermediate water salinity. Because the changes in density largely depend on salinity in this run, and the dip in marginal temperature also slightly leads the precession minimum, 370 it follows that the midpoint of this time interval of minimal DWF falls prior to the precession minimum.

375 The DWF does not stop completely in this run (see Fig. 3E), because the relatively warm open Mediterranean surface/intermediate water keeps the deep water warmer (through mixing) than the marginal water, see Fig. 3. This reference run highlights why the sapropel state is inherently transient: the DWF is only slowed down when the density of the upper boxes is decreasing, and increases again when the density starts to return to precession maximum conditions. Since density cannot decrease indefinitely, 380 a state with minimum circulation cannot be maintained.

385 The deep water flux at the precession maximum ( $3 \cdot 10^5 \text{ m}^3/\text{s}$ ) is somewhat lower than found in observational data ( $3-10^5 \text{ m}^3/\text{s}$  versus approximately  $(1.6-10^6 \text{ m}^3/\text{s})$  ( $1.6 \cdot 10^6 \text{ m}^3/\text{s}$ , Pinardi et al., 2015)), although comparable to the DWF of one of the Eastern sub-basins sub-basins (Pinardi et al., 2015). Deep water oxygen is within error of the actual value ( $181 \mu\text{M}$  in the model versus between 155 and  $205 \mu\text{M}$  observed in the Western 390 . Other conditions, such as temperature and salinity match closely to present day winter conditions (as reported in Hayes et al., 2019). DWF only occurs at the margins (box 1) in this run, the other deep water flux is only plotted for easy comparison to other runs (in which it does occur). None of the fluxes change direction in this run, resulting in relatively simple, although not entirely linear behaviour: the phase relation between the salinities of the boxes is not constant, and the temperature of the marginal box, as well as the deep water oxygen curve are clearly not sinusoidal. We consider the period with minimal deep water oxygen concentration,  $60 \mu\text{M}$ , to be the model equivalent of sapropel conditions. Although we only find a very short sapropel, (from 8.8 – 10.3 kyr) this run demonstrates that the model (i) is capable of approximating the present-day water properties and circulation when forced by present atmospheric conditions, and (ii) captures the reduction in DWF expected upon a change to wetter conditions.

### 3.2 Addition of atmospheric temperature variability

395 As described in the introduction, temperature variation due to precession likely also affected buoyancy loss. In order to examine this aspect, we run the model with a  $3^{\circ}\text{C}$  temperature increase at the precession minimum relative to the precession maximum. For atmospheric box  $\text{A1}$ – $\text{A}_1$  the temperature increases from 12 to  $15^{\circ}\text{C}$ , and for box  $\text{A2}$ – $\text{A}_1$  the temperature increases from 10 to  $13^{\circ}\text{C}$ . Both air temperature curves are described by sine waves, as shown in Fig. 4C. We decide to maintain a constant temperature difference between the two atmospheric boxes as there is insufficient evidence for other options. All other parameters  
400 are set as described in the reference run.

The overall behaviour of the model is similar to that in the reference run, except that the temperatures of all boxes are now higher during the interval surrounding the precession minimum (Fig. 4C). We still observe a minor decrease in marginal water temperatures at the precession minimum (cf. Fig. 3C), albeit much smaller than in the reference run, since it is now imposed on top of the trend caused by the changing atmospheric temperature. The net effect of a homogeneous basin wide temperature  
405 increase during the precession minimum is a further decrease in DWF during this time interval. We find a sapropel from  $t=2900$  years to  $6500$ – $8084$  years to  $10970$  years, which therefore lasts  $3600$ – $2013$  years and the midpoint leads the precession minimum by  $300$ – $473$  years (see Fig. 4E).

When testing the parameter space, we find that changes in marginal and open Mediterranean air temperature have an opposite effect on DWF: when the air over the margins becomes warmer, heat exchange with the marginal water directly increases the  
410 buoyancy of the water involved in DWF, slowing the circulation down. An increase in open Mediterranean air temperature, in contrast, primarily affects the open Mediterranean surface/intermediate water, which mixes with the deep water over a large area. The resulting rise in temperature of the deep water lowers its density, and thereby increases the marginal to deep water density gradient. Since this gradient controls DWF formation at the margin, an increase in open Mediterranean air temperature  
415 ultimately causes an increase in DWF. Since part of the open Mediterranean surface/intermediate water flows to the and mixes with the marginal water, the effect of the open Mediterranean air temperature increase on the margin-deep water density gradient is relatively small.

This run shows that an atmospheric temperature ~~increases~~ increase during the precession minimum significantly affects the duration of sapropel conditions in the model. Since both observational and modelling studies find this temperature variability (Marzocchi et al., 2015; Herbert et al., 2015), it will be included in all following model runs.

### 420 3.3 Nonlinear behaviour

Next, we explore the effect of a transition to and from a time interval with a positive freshwater budget. Whether or not the  
425 freshwater budget of the Mediterranean Sea becomes positive during sapropel formation has been widely debated (Rohling, 1994, and references therein). Although our model cannot directly prove whether or not this has happened, it does allow us to study what the implications for the water properties and circulation would be, which should help in recognising the expression of a budget switch in the geological record. First we consider a scenario where only the freshwater budget of the margins

becomes positive; in a subsequent run we force the model in such a way that the freshwater budget of the entire basin changes sign.

To have the freshwater budget of the margins become positive, the maximum ~~outflow of river 1 of  $R_1$~~  is increased from  $6.7 \cdot 10^3$   $1.2 \cdot 10^3$   $m^3/s$  to  $1.4 \cdot 10^4$   $m^3/s$  (Fig. 5A). All other parameters are kept the same as in the temperature variability run (Fig. 4).

At a similar timing as the dip in temperature observed in the reference run, we now see a very large decrease in salinity at the margins from 9 to 13 kyr (see Fig. 5B). During this interval we observe that temperatures at the margins approach the temperature of the overlying atmospheric box, while deep water temperatures approach those found in the open Mediterranean (see Fig. 5C). All are an ~~expression~~ expression of the disappearance of DWF at the margin (see Fig. 5DE; elaborated below) which effectively stops the exchange of the margins with the rest of the basin. Conditions at the margins are mainly determined by the river input (causing low salinity) and atmospheric temperature. The properties of the deep water are now only determined by mixing with the open Mediterranean surface/intermediate box, and DWF in the same box, explaining the similar temperatures.

When the salinity at the margins ~~reach normal reaches present day~~ values again at 13 kyr, we observe a sudden subtle increase in deep water salinity, due to the abrupt increase in DWF at the margin at this moment (see Fig. 5D).

Because the change in salinity is much larger than the change in temperature, the densities of each of the boxes (Fig. 5D) behave similarly to the observed salinities seen in Fig. 5B.

DWF at the margins is found to gradually decrease towards the precession minimum, then completely stop at around 8 kyr, and abruptly increase to normal circulation again at around 13 kyr. DWF in the open Mediterranean starts close to the precession minimum and ends abruptly when DWF at the margins starts again. Deep water oxygen largely ~~behaves as correlates with~~ the total DWF, although it reaches a minimum before DWF stops completely and begins to increase only shortly after DWF in the open Mediterranean starts. Similar to previous runs, outflow to the Atlantic (Fig. 5E) is slightly lower during the precession minimum, because 1(i) the density difference between the Atlantic and open Mediterranean surface/intermediate box is smaller, and 2(ii) the freshwater budget is closer to zero.

We thus find that when the freshwater budget in the marginal box temporarily becomes positive, DWF occurs in the open Mediterranean at the end of the low deep water oxygen interval (conditions associated with sapropel deposition), thereby terminating this interval early (as shown in Fig. 5). Deep water mixing with the much less dense water at the margins decreases the density of the deep water, thereby causing DWF in the open Mediterranean box. The result of this is a phase lead of the sapropel midpoint (as a result of the earlier termination), instead of a phase lag commonly reported in literature (Grant et al., 2016).

In the next run we force the model in such a way that the freshwater budget of the entire basin becomes positive during the interval straddling the precession minimum.

The maximum ~~outflow of river 2 of  $R_2$~~  is set to  $8 \cdot 10^4$   $m^3/s$  and the minimum evaporation to 0.74 m/yr (Fig. 6A), all other parameters are kept the same as in the temperature variability run. In the interval from approximately 9 to 13 kyr, the freshwater budget of the entire basin reverses.

460 Salinities (Fig. 6B) ~~decreases~~ decrease in response to the decrease in net evaporation. When the freshwater budget reverses, the exchange with the Atlantic decreases, causing less relatively saline water to flow into the upper boxes. Consequently, the salinity of the upper boxes further decreases. The deep water salinity only begins to decrease more when DWF at the margin starts again. When the freshwater budget becomes negative again, the salinities abruptly increase and then follow the freshwater budget more or less linearly.

465 The main features of the temperature curves (Fig. 6C) are caused by the same events that are described above for the salinity variability, although temperature is also affected by heat loss to the atmosphere. Consequently, the same main features can be identified, with the difference that 1) the temperature of the upper boxes follows the air temperature curves, and 2) the amplitude is smaller, because the heat exchange with the atmosphere acts as negative feedback.

470 The changes in densities are predominantly determined by salinity, as the changes in temperature are relatively small in this run.

Reversing the freshwater budget also causes the density difference between the Atlantic and open Mediterranean surface/intermediate box to change sign. Consequently, the density driven flow goes from the Atlantic to the Mediterranean, instead of the other way around. In Fig. 6E, this is represented by the flux becoming negative. Note that this shift occurs almost instantaneously.

475 In this run, we find a very sharp termination of the sapropel, followed by a brief period with lower oxygen concentration (as shown in Fig. 6). This is caused by a peak in DWF in both the margin and open Mediterranean when the freshwater budget changes sign. Just prior to the reversal of the freshwater budget, the density of the open Mediterranean surface/intermediate water is much lower than that of the Atlantic water. The reversal of the freshwater budget then causes a rapid increase in surface/intermediate water throughout the basin, resulting in the peak in DWF.

480 The irregularities observed in all runs (such as the occurrence of multiple local minima) where the freshwater budget of (part of) the basin reverses all strongly depend on the model set-up.

### 3.4 Phase of evaporation

Recent modelling studies (Marzocchi, 2016) have shown that while evaporation and river outflow are both forced by precession, they may have a different phase relation to their forcing. Runoff and evaporation are the only transient forcings in the presented model runs, therefore shifting runoff for example 2 kyr forward in time gives the exact same wave shape as shifting evaporation 2 kyr backwards in time. The only difference would be that the waveform would be shifted by 4 kyr. Since we are primarily interested in the transient response rather than the absolute timing, we only investigate the effect of the phase of evaporation. To assess the effect of the phase of evaporation on sapropel formation, we calculate the sapropel midpoint and duration for a set of runs, with varying evaporation phase (all other parameters remaining unaltered between runs). Apart from the phase 490 of the evaporation forcing, the model is forced exactly the same as in the atmospheric temperature variability experiment (as described in subsection 3.2).

As shown in Fig. 7, we find a maximum in sapropel duration when evaporation is almost in phase with precession. This is to be expected, as minimum evaporation then coincides with maximum river outflow. Similarly, a minimum in sapropel duration

is found when evaporation is almost exactly in anti-phase with precession. In between these peaks the sapropel duration as a  
495 function of the phase of evaporation is described by a cosine. The sapropel midpoint is found to vary significantly (~~hundreds up~~  
to thousands of years with a large amplitude of evaporation variability) when varying the phase of the evaporation forcing. The  
shift in sapropel midpoint relative to the precession minimum is at a maximum when evaporation lags or leads approximately  
5 kyr. This makes sense, as the minimum in midpoint shift occurs when evaporation is either in phase with precession, or in  
500 anti-phase (i.e. a shift of 0 or 10 kyr), the 5 kyr lead/lag falls right in between these points. The timing of the midpoint as a  
function of the phase of evaporation in between these extremes is described by a nearly perfect sine wave. Note that the peaks  
are not exactly at -5 and 5 kyr, but slightly shifted, this is likely a result of the equilibrium time of the system.

This experiment, combined with the systematic testing of the parameter space, highlights that although the exact timing and duration depend on the exact forcing, the minimum in deep water oxygen concentration always occurs close to the precession minimum and the model response is always quasi-linear, as long as fresh water budgets are not reversed.

505 We also find that the magnitude of the effect of the phase of evaporation on sapropel timing and duration depends on the amplitude of the evaporation variability (not shown). This makes sense, as the changes in circulation largely respond to freshwater budgets (the only difference between river inflow and evaporation being their respective temperatures) and the amplitude of evaporation variability scales linearly with its impact on the variability of the freshwater budgets.

When systematically varying the components of the water budget within the limits mentioned in model setup, we find that  
510 in the regimes where the freshwater budget of (part of) the basin changes sign, sapropels are cut short considerably. When performing the same analyses described above, but now using the forcing of the first run in subsection 3.3, we find that this causes the midpoint of the sapropel to occur prior to the precession minimum (Fig. 8). Note that runs with multiple sapropel intervals cannot be described as having a single midpoint or duration.

## 4 Discussion

### 515 4.1 Statistical analysis Model convergence

One of the results of the model is that slight variations of forcing parameters can cause significantly different sapropel duration and timing. We therefore introduce a statistical test to determine the magnitude thereof, given the uncertainty of each of the forcing variables. With eleven forcing parameters (the phase of evaporation and minima and maxima of R1, R2, TA1, TA2 and evaporation) it is not feasible to calculate all permutations at a meaningful resolution. We therefore randomly pick and run 200  
520 permutations (fewer permutations would produce unreliable results), given the uncertainty of each parameter, and calculate the  $1\sigma$  and minimum and maximum values of the resulting oxygen concentrations per time step (see Fig. A1 for an example). During testing, we can thereby visualize much more of the parameter space than when doing individual runs.

### 4.2 Model convergence

525 The annual resolution The time step of one year naturally results from the concept that deep water forms during winter storms, making it the highest resolution possible as long as seasonal variability is not included. From a purely mathematical perspective, however, the time resolution should not affect the outcome significantly, as long as a sufficiently small time step is used to prevent aliasing. We tested this by varying the temporal resolution given a certain forcing. We find that no significantly different results with a time step below 6 years, the only difference in the model results (compared to the result when using a higher temporal resolution) is in the fluctuation around an oxygen concentration of  $60 \mu M$ , during sapropelic conditions. This 530 fluctuation scales linearly with the time step, with an amplitude of approximately  $0.4 \mu M$  at 10 years. With a time step of 1 year and  $0.04 \mu M$  at a time step of 1/10th of a year, see Fig. ??, larger than 10 years aliasing occurs. We conclude that a time step of 1 year is sufficient for the analyses in the this study.

## 4.2 The role of assumptions and simplifications

535 All models require assumptions and simplifications to be made, as they are by design a simplified version of (part of) a system. Simple box models, such as the model presented in this paper, aim to identify the smallest subset of processes that can describe a certain phenomenon. As such, this model represents a generic semi-enclosed basin, given that no specific geometry is included. This also implies that by altering the parameter values and in some cases the strait exchange equations, the model can easily be adapted to other semi-enclosed basins, such as the Black Sea.

540 In our model we parametrize intra-annual variability. Including seasonality would require separate intermediate water boxes (increasing complexity), while for the oxygenation of deep water only the amount of DWF and mixing with the overlying water mass is truly relevant. Furthermore, we would have to make assumptions regarding the annual variability of the forcing parameters (river outflow and evaporation), which are not well constrained for geological history. We therefore decided to parameterize the seasonal variability, by calculating a yearly averaged DWF flux based on winter temperatures. This allows us 545 to study the fundamental mechanisms of sapropel formation. OGCMs would be more appropriate to study the role of seasonal variation.

550 We do not include separate boxes for the Eastern and Western Mediterranean in our model. The aim of a conceptual model is to capture the first order aspects of a process with a minimal setup. The current setup does this. Incorporating separate sub-basins would imply doubling the number of boxes and would also double the number of forcing parameters and equations, all of which add uncertainty to the model (quantitative reconstructions do not exist for most of these parameters). Moreover, the complexity quickly increases, making it much harder to test and describe the parameter space and identify key mechanisms. While this could be tested in a future study, we find it important to first understand the behaviour of the a semi-enclosed basin with a gateway before studying what is essentially a second order system. We expect that the effect in the Eastern basin is similar to the difference between a first order and second order filter: a larger shift of the midpoint (larger group delay), and likely a higher sensitivity in the Eastern basin. Any resonances in the system are also expected to become more prominent 555 (since the resonant frequencies are now amplified twice).

The model forcing used in this study is chosen to reflect either the variability described by the main hypothesis envisaged in the commonly accepted mechanism (as sketched in subsection 1.1), or oceanographic and climatic variability deduced from

modelling studies and the geological record as ~~aeccurate~~accurately as possible. Other processes such as the North Atlantic oscillation and solar activity are not taken into account, because they are not thought to be of first order importance for 560 sapropel formation, as described in Rossignol-Strick (1985) and Rohling et al. (2015), for example. While these processes likely influence sapropel formation, they are unlikely to be essential. Besides precession, obliquity also affects sapropel formation, but it is not our aim to reconstruct the exact conditions during specific time intervals. For an individual sapropel, adding an obliquity component would effectively slightly modulate the frequency and amplitude of the forcing. Since the model is not very sensitive to the exact frequency of the forcing, and we already extensively tested the parameter space in terms of 565 amplitude, a simple (20 kyr) sine wave suffices as forcing. Also note that since obliquity does not have a harmonic relation with precession, the modulation would not have the same effect on every sapropel. It likely affects the thickness of a sapropel for example, but the effect may work both ways when comparing different sapropels.

The model output comprises an average value for deep water oxygen, as the deep water is a single box. In reality, however, oxygen concentrations vary spatially. A prime example of ~~thereof~~this is the absence of sapropels in most of the Western 570 Mediterranean Sea. This abstraction should be taken into consideration when interpreting the model results. This model focuses on the transient response of water fluxes in the Mediterranean Sea, the oxygen output is calculated to get a first order impression of deep water ventilation. A biogeochemical model, ~~comparable similar~~ to the one presented in ~~(Slomp and Van Cappellen, 2007)~~ Slomp and Van Cappellen (2007), would have to be included to specifically study bottom water oxygenation. We expect that the main difference with a biogeochemical model ~~will be is~~ that in our model river input directly affects oxygen consumption, 575 while the surface/intermediate boxes would act as a reservoir for nutrients (with their own feedbacks) in the biogeochemical model.

, thereby delaying the response to changes in river input. Note finally that in reality DWF occurs following two different mechanisms ~~-(open ocean convection and mixing of the water at margins during winter storms, which then cascades to the deep basin, see subsection 1.1),~~ as well as in multiple ~~sub-basins~~sub-basins that each have their own conditions.

580 The regime in Fig. 5 relies on the freshwater budget of the margins changing sign. In reality there are many different marginal water masses in the sub-basins, rather than one single "margin". This makes it likely that the freshwater budget becoming positive in any one of these sub-basins will have similar consequences for the circulation. Since the freshwater budgets of these basins are independent, it would be possible to drastically alter the circulation multiple times during a single precession cycle. Presently, the Adriatic sea has a positive freshwater budget (Raicich, 1996), and the Aegean sea is known to have had a positive 585 fresh water budget in the past (Zervakis et al., 2004).

The simplicity of the model makes it especially suitable for describing transient, nonlinear behaviour, allowing for the identification of crucial mechanisms. More complex models, while providing other benefits, are generally too difficult to interpret on this level, or do not allow for runs of sufficient length to study the transient response over a full precession cycle. The presented model runs give an overview of the behaviour of the model. When systematically testing the parameter space, 590 we find that this behaviour largely depends on general trends and reversal of fresh water budgets, rather than specific forcing or parameter choices. This makes the results of the study much more robust and meaningful.

595 Exchange with the Black Sea also affects circulation in the Mediterranean Sea (Soulet et al., 2013, show increased runoff during HS1). For sapropels during which there is exchange through the Bosphorus strait, the exchange is not constant through time, and also depends on the inflow of Mediterranean water into the Black Sea. Opening or closing of the strait prior to, or during, a sapropel 595 may impact the circulation. When the sill becomes deep enough to allow for a two layer exchange, a large amount of saline water would flow into the Black Sea (following the same principle as at the Gibraltar Strait), thereby causing extra, relatively 600 fresh, water to flow out into the Mediterranean Sea. During some sapropels, the strait may have been closed. Furthermore, there is very little data regarding the exchange opening and closing of the Bosphorus Strait prior to the most recent opening (approximately 11 ka), perhaps with the exception of the Pontian (which is beyond the scope of this paper). Consequently, we 600 do not include exchange with the Black Sea. For the cases where there was a steady outflow of fresh water (or an exchange that can be parametrized as such) this could indeed be seen as an extra fresh water source for the margins. We have already tested this effect by varying the river outflow into the margins.

605 Melt water pulses likely affect sapropel formation, but we do not consider them to be of first order importance. During many sapropels, melt water pulses did not occur. In future applications of this model where a specific sapropel/interval is studied, drivers such as melt water pulses should be included.

### 4.3 Describing nonlinear relationships and transient response

610 The occurrence of sapropels is often considered from a binary perspective: a sediment is either a sapropel, or it is not. The dominant forcing mechanism (astronomic variability), however, can be easily described by a combination of a limited number of sine-waves: the resonant frequencies of the planetary bodies in our solar system (for example Laskar, 1988). For a single 610 sapropel, only climatic precession—a nearly a perfect sine—is considered to be of first order importance in controlling bottom water oxygenation (Rossignol-Strick, 1985), with the rest of the orbital configuration mostly modulating the effect of precession. If a model strives to capture the current hypothesis of sapropel formation, starting from astronomic variability, it must therefore transform a sine wave into something that is not a sine wave, requiring the model to be nonlinear. Our model allows 615 for such behaviour. Even when considering intra-sapropel variability, thereby surpassing a binary approach, the sapropel record is clearly not sinusoidal (see for example Grant et al., 2016; Dirksen et al., 2019).

620 One of the main research questions of this study is when sapropel formation occurs. In a linear system, one would simply calculate the phase of the output with respect to the input. However, as the output is no longer linearly related to the input, this is not possible. A simple threshold ~~analyses will not suffice~~ analysis is not ideal either, as the cut-off level can have major impact on both timing and duration, while a clear definition is not readily available. Furthermore, even when the threshold is 620 defined, this method would not be usable for sapropelic marls, which are thought to be the result of the same process, but do not share the same chemical composition. We partly avoid this problem by ~~instead not only~~ considering the midpoint of the sapropel (when assuming a certain oxygen threshold, see subsection 4.4). ~~While this can't be related directly 4.5), but also the full wave form (e.g. which intervals could be sapropelic with a slightly different forcing). In the sedimentary record this is generally not possible, since the non-sapropelic intervals do not record all parameters and are often bioturbated. So while our approach cannot be applied~~ to the sedimentary record, it does give insight into ~~factors~~ the factors that influence sapropel

timing. Even this definition of sapropel timing becomes problematic when one or more interruptions occur, since in that case there is more than one ~~mid-point~~midpoint.

We find that, when using realistic model forcing, stable sapropel conditions do not occur. Even when using constant forcing, a permanent complete stop of DWF either does not occur, or only under very specific conditions. Note that in the Black Sea 630 permanent stratification does appear to occur, ~~however~~but here, the positive freshwater budget allows some of the water flowing into the Black Sea at the Bosphorus Strait to sink to the deep water (Bogdanova, 1963), keeping it relatively saline and dense. However, our results indicate that sapropel conditions can occur transiently without a positive freshwater budget, with realistic forcing. We therefore conclude that studying the oceanographic state during sapropel conditions by modelling steady-state conditions with a stratified water column results in a very limited understanding of sapropel formation.

#### 635 4.4 Comparison with geological data and other models

Comparing model results to geological data is most effective when an accurate age model is available for the geological data. We will therefore only consider the ~~five~~5 youngest sapropels in this paper. The most recent sapropel (S1) is thought to have been triggered by sea level rise, which in turn resulted in a connection between the Black Sea and the Mediterranean Sea (Rohling et al., 2015). As both sea level variability and exchange through the ~~Bosphorus~~Bosphorus Strait are beyond the scope of this 640 paper, sapropel S1 is not suitable for comparison. We therefore focus on sapropels S3, S4, and S5 in the rest of the section.

In the run with variable air temperature (Fig. 4), the modelled sapropel duration and timing is within ~~error~~dating uncertainty with what has been found for sapropel S3 and S4 in core LC21 (Grant et al., 2016). Note that the same study finds that sapropels S1 and S5 lag precession by 2.1–3.3 kyr. This suggests that our model is capable of capturing the most relevant mechanisms for S3 and S4, but that other features not included in the model affected the timing of S1 and S5. For S5 there is evidence 645 suggesting that the Black Sea reconnected to the Mediterranean Sea within the ~~dating~~ uncertainty of the onset of sapropel S5 (Grant et al., 2016, 2012; Wegwerth et al., 2014)

It should be noted that while the model often shows a midpoint lag (relative to the insolation minimum) of a few hundred years, uncertainties related to radiometric dating methods are often larger. However, we find that midpoint lag becomes larger with decreasing strait efficiency, implying that during times with low sea level or otherwise restricted exchange, the lag might 650 become very relevant. A prime example of such a case would be the Messinian Salinity crisis and the surrounding intervals (Topper and Meijer, 2015). Moreover, as shown in Figures 5 and 6, ~~the alternative regimes~~alternative regimes (where the freshwater budget of either part of the basin, or the entire basin changes sign) can shift the midpoint of the sapropel considerably, as shown in Fig. 8. Unlike the relatively minor shifts in midpoint resulting from only changing the phase of evaporation, the resulting difference in sapropel timing is sufficiently large to be detectable in the geological record.

655 De Lange et al. (2008) find that the freshening of the surface waters starts earlier and lasts longer than the suboxic bottom water conditions during S1. Our model also shows this behaviour in all of the presented runs (most notably in figures 3, 4 and 6). This makes sense, as the DWF does not stop completely when the surface water starts to become less saline; it only reduces slowly. Furthermore, the oxygen has to be depleted for suboxic condition to occur, this is limited by oxygen consumption, and further slowed down by vertical mixing and DWF. How much longer the period of reduced sea surface salinity lasts compared

660 to the period of suboxic bottom water likely depends on the exact location and water depth. The model is therefore mostly useful to gain insight into the mechanisms, rather than in the exact timing.

The regime described in Fig. 6 can show a sudden termination of the sapropel, which is similar to that seen in records of sapropel S5 (Dirksen et al., 2019). In the model, such a sudden termination can only be achieved by forming deep water in the open Mediterranean, by reversereversing the freshwater budget of the entire Mediterranean. The coupling between the margins and deep water is insufficient to cause such a sudden termination. This suggests that during S5 the freshwater budget of part of the basin, or the whole basin potentially reversed. Such a large change in freshwater budget is in line with Bale et al. (2019), who found that surface salinities in three different cores in the eastern Mediterranean were sufficiently low to support free-living heterocystous cyanobacteria during sapropel S5. Moreover, oceanographic conditions may differ significantly between different parts of the basin: the oxygen concentration (and related variables) of a hypothetical core taken at the margin would 670 be expected to show a pattern more similar to the DWF in the marginal box, while a core in the open Mediterranean may be more similar to the open Mediterranean surface/intermediate water box.

Sapropel interruptions commonly occur in the stratigraphic record (for example in S5 in core LC21, Rohling et al., 2006, 2015). With slightly different settings, the sharp peak in deep water oxygen in Fig. 6E can be made to occur earlier and less intense, resulting in an interrupted sapropel. The model therefore suggests that such interruptions can occur without further 675 external forcing. This hypothesis could be tested in the stratigraphic record by looking for evidence of a reversed freshwater budget of (part of) the basin during such interrupted sapropels, and constructing high resolution intra-sapropel age models to assess the relative timing of the relevant features compared to insolation.

Each sapropel in the geological record is different, this already becomes apparent when considering the first sixmost recent 6: S1 has a different timing and is likely related to sea level variability (Grant et al., 2016; Hennekam, 2015)(Grant et al., 2016; Hennekam, 2015). S2 is not found at all. S4 has an interruptionand interruptions in core LC21 (Grant et al., 2012), and the high resolution records 680 of for example trace metals show very different characteristics. In the same core, the timing of the midpoint of S3 and S4 compared to insolation is the same, while that of S1 and S5 are different. S5 is much longer than all of the previous sapropels, does not have any burn down at at least one location (Dirksen et al., 2019), has an interruption in other locations (Rohling et al., 2006) and again shows generally different characteristics in different cores (Dirksen et al., 2019; Grant et al., 2016; Rohling et al., 2006). S6 again looks very different.

We conclude that both in the geological record and in the model, a typical sapropel does not exist. The timing and mechanisms involved may differ considerably between sapropels and locations, as highlighted by our model results. Moreover, we find that an increase in freshwater budget alone is not sufficient to describe all key aspects of sapropel formation. An increase in atmospheric temperatures during the precession minimum (as observed in data and modelling studies Marzocchi et al., 2015; Herbert et al., 2015) 690 (as observed in data and modelling studies, Marzocchi et al., 2015; Herbert et al., 2015) directly affects buoyancy loss during the interval in which sapropels form. This makes atmospheric temperature variability an integral feature of the system, without Without it unrealistic evaporation or river outflow is needed to result in sufficiently long sapropels. Our model results support this hypothesis.

## 5 Conclusions

695 The analysis presented in this paper illustrates that relatively simple models can give new, fundamental insights into the physical processes driving sapropel formation. The timing of sapropels relative to insolation has been widely studied in the sedimentary record. On the basis of our novel long-duration experiments we find that the timing of sapropels is very sensitive to the exact climatologic and oceanographic conditions.

700 The nonlinear response to insolation forcing implies that the sapropel record does not have a linear phase relation with insolation. The strongly nonlinear regimes in our model highlight that the mid-point of a sapropel (the average of the ages of the top and bottom of the sapropel) can be shifted significantly with a minor change in forcing, by cutting it short with a sudden termination, while during the rest of the precession cycle the response can be very similar to the nearly linear regime presented in the reference experiment.

705 Our model results suggest that an increase in freshwater input alone, as in the general hypothesis for sapropel formation, does not provide a sufficient reduction in buoyancy loss to form sapropels as they are found in the geological record. We propose that precession controlled atmospheric temperature variability also plays a key role in the process of sapropel formation.

## Appendix A: Appendix A

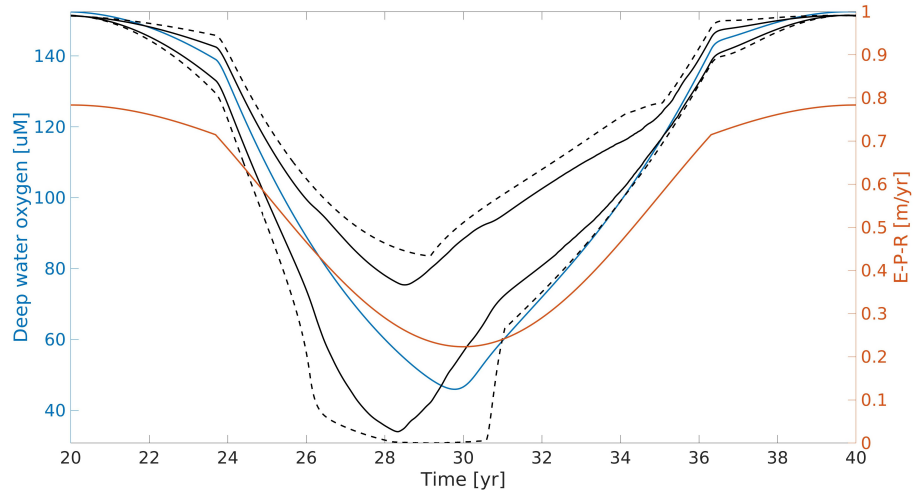


**Figure A1.** An example of the sensitivity analyses. Here the maximum of  $R1 + R2$  is varied randomly by up to  $5 \cdot 10^3 \text{ m}^3/\text{s}$  above or below the general setting over 200 runs. The solid lines blue line indicate the general initial run, the blue dashed solid black lines indicate the upper and lower  $1\sigma$  of each point in time, and the black dashed lines the minimum and maximum.

### A1

710 *Author contributions.* P. Meijer conceived the basic idea. J.P. Dirksen elaborated the concepts and performed the analyses. Both authors contributed to the model set-up and the writing of the manuscript.

*Competing interests.* The authors have no competing interests.

*Acknowledgements.* This work was financially supported by The Netherlands Research Centre for Integrated Solid Earth Science (ISES 2017-UU-23). The Authors would like to thank Ronja Ebner for the many useful discussions and her help with checking the formulas.

Adloff, F., Mikolajewicz, U., Kučera, M., Grimm, R., Maier-Reimer, E., Schmiedl, G., and Emeis, K. C.: Upper ocean climate of the Eastern Mediterranean Sea during the Holocene Insolation Maximum - A model study, *Climate of the Past*, 7, 1103–1122, <https://doi.org/10.5194/cp-7-1103-2011>, 2011.

Amies, J., Rohling, E. J., and Grant, K. M.: Quantification of African Monsoon Runoff During Last Interglacial Sapropel S5, *Paleoceanography and Paleoclimatology*, pp. 1–30, <https://doi.org/10.1029/2019PA003652>, 2019.

Ashkenazy, Y., Stone, P. H., and Malanotte-Rizzoli, P.: Box modeling of the Eastern Mediterranean sea, *Physica A: Statistical Mechanics and its Applications*, 391, 1519–1531, <https://doi.org/10.1016/j.physa.2011.08.026>, <http://dx.doi.org/10.1016/j.physa.2011.08.026>, 2012.

Bale, N. J., Hennekam, R., Hopmans, E. C., Dorhout, D., Reichart, G.-j., Meer, M. V. D., Villareal, T. A., Damsté, J. S. S., and Schouten, S.: Biomarker evidence for nitrogen-fixing cyanobacterial blooms in a brackish surface layer in the Nile River plume during sapropel deposition, *Geology*, XX, 1–5, <https://doi.org/10.1130/G46682.1/4834380/g46682.pdf>, 2019.

Bensi, M., Cardin, V., Rubino, A., Notarstefano, G., and Poulain, P. M.: Effects of winter convection on the deep layer of the Southern Adriatic Sea in 2012, *Journal of Geophysical Research: Oceans*, 118, 6064–6075, <https://doi.org/10.1002/2013JC009432>, 2013.

Bianchi, D., Zavatarelli, M., Pinardi, N., Capozzi, R., Capotondi, L., Corselli, C., and Masina, S.: Simulations of ecosystem response during the sapropel S1 deposition event, *Palaeogeography, Palaeoclimatology, Palaeoecology*, 235, 265–287, <https://doi.org/10.1016/j.palaeo.2005.09.032>, 2006.

Bigg, G. R.: An ocean general circulation model view of the glacial Mediterranean thermohaline circulation, *Paleoceanography*, 9, 705–722, <https://doi.org/10.1029/94PA01183>, 1994.

Bogdanova, A. K.: The distribution of Mediterranean waters in the Black Sea, *Deep-Sea Research and Oceanographic Abstracts*, 10, 665–672, [https://doi.org/10.1016/0011-7471\(63\)90014-7](https://doi.org/10.1016/0011-7471(63)90014-7), 1963.

Bryden, H. L. and Kinder, T. H.: Steady two-layer exchange through the Strait of Gibraltar, *Deep Sea Research Part A. Oceanographic Research Papers*, 38, S445–S463, [https://doi.org/10.1016/s0198-0149\(12\)80020-3](https://doi.org/10.1016/s0198-0149(12)80020-3), 1991.

Calvert, S. E., Nielsen, B., and Fontugne, M. R.: Evidence from nitrogen isotope ratios for enhanced productivity during formation of eastern Mediterranean sapropels, *Nature*, 359, 223–225, <https://doi.org/10.1038/359223a0>, 1992.

Channell, J. E. T., Hodell, D. A., Singer, B. S., and Xuan, C.: Reconciling astrochronological and  $^{40}\text{Ar}/^{39}\text{Ar}$  ages for the Matuyama-Brunhes boundary and late Matuyama Chron , *Geochemistry, Geophysics, Geosystems*, 11, n/a–n/a, <https://doi.org/10.1029/2010gc003203>, 2010.

Command, N. O.: US Navy climatic study of the Mediterranean Sea, Naval Oceanography Command Detachment, Asheville, North Carolina (342 pp.), 1987.

Cramp, A. and O’Sullivan, G.: Neogene sapropels in the Mediterranean: A review, *Marine Geology*, 153, 11–28, [https://doi.org/10.1016/S0025-3227\(98\)00092-9](https://doi.org/10.1016/S0025-3227(98)00092-9), 1999.

De Lange, G. and Ten Haven, H.: Recent sapropel formation in the eastern Mediterranean, *Nature*, 305, 797, 1983.

De Lange, G. J., Thomson, J., Reitz, A., Slomp, C. P., Speranza Principato, M., Erba, E., and Corselli, C.: Synchronous basin-wide formation and redox-controlled preservation of a Mediterranean sapropel, *Nature Geoscience*, 1, 606–610, <https://doi.org/10.1038/ngeo283>, 2008.

Dirksen, J. P., Hennekam, R., Geerken, E., and Reichart, G. J.: A Novel Approach Using Time-Depth Distortions to Assess Multicentennial Variability in Deep-Sea Oxygen Deficiency in the Eastern Mediterranean Sea During Sapropel S5, *Paleoceanography and Paleoclimatology*, 34, 774–786, <https://doi.org/10.1029/2018PA003458>, 2019.

Finnigan, T. D., Winters, K. B., and Ivey, G. N.: Response Characteristics of a Buoyancy-Driven Sea, *Journal of Physical Oceanography*, 31, 2721–2736, [https://doi.org/10.1175/1520-0485\(2001\)031<2721:RCOABD>2.0.CO;2](https://doi.org/10.1175/1520-0485(2001)031<2721:RCOABD>2.0.CO;2), 2001.

Gertman, I., Pinardi, N., Popov, Y., and Hecht, A.: Aegean sea water masses during the early stages of the Eastern Mediterranean Climatic  
755 Transient (1988–90), *Journal of Physical Oceanography*, 36, 1841–1859, <https://doi.org/10.1175/JPO2940.1>, 2006.

Gertmann, I., Ovchinnikov, I., and Popv, Y.: Deep convection in the eastern basin of the Mediterranean Sea, *Oceanology*, 34, 19–25, 1994.

Grant, K. M., Rohling, E. J., Bar-Matthews, M., Ayalon, A., Medina-Elizalde, M., Ramsey, C. B., Satow, C., and Roberts, A. P.: Rapid coupling between ice volume and polar temperature over the past 50,000 years, *Nature*, 491, 744–747, <https://doi.org/10.1038/nature11593>, 2012.

760 Grant, K. M., Grimm, R., Mikolajewicz, U., Marino, G., Ziegler, M., and Rohling, E. J.: The timing of Mediterranean sapropel deposition relative to insolation, sea-level and African monsoon changes, *Quaternary Science Reviews*, 140, 125–141, <https://doi.org/10.1016/j.quascirev.2016.03.026>, <http://dx.doi.org/10.1016/j.quascirev.2016.03.026>, 2016.

Grimm, R., Maier-Reimer, E., Mikolajewicz, U., Schmiedl, G., Müller-Navarra, K., Adloff, F., Grant, K. M., Ziegler, M., Lourens, L. J., and Emeis, K. C.: Late glacial initiation of Holocene eastern Mediterranean sapropel formation, *Nature Communications*, 6, 765 <https://doi.org/10.1038/ncomms8099>, 2015.

Hayes, D. R., Schroeder, K., Poulain, P.-M., Testor, P., Mortier, L., Bosse, A., and du Madron, X.: 18 Review of the Circulation and Characteristics of Intermediate Water Masses of the Mediterranean: Implications for Cold-Water Coral Habitats, -, 9, 195–211, [https://doi.org/10.1007/978-3-319-91608-8\\_18](https://doi.org/10.1007/978-3-319-91608-8_18), 2019.

Hennekam, R.: High-frequency climate variability in the late Quaternary eastern Mediterranean Associations of Nile discharge and basin  
770 overturning circulation dynamics, no. 78 in *Utrecht Stud. Earth Sci.*, UU Dept. of Earth Sciences, 2015.

Herbert, T. D., Ng, G., and Peterson, L. C.: Evolution of Mediterranean sea surface temperatures 3.5–1.5 Ma: regional and hemispheric influences, *Earth and Planetary Science Letters*, 409, 307–318, 2015.

Herrmann, M., Estournel, C., Déqué, M., Marsaleix, P., Sevault, F., and Somot, S.: Dense water formation in the Gulf of Lions shelf: Impact of atmospheric interannual variability and climate change, *Continental Shelf Research*, 28, 2092–2112, 775 <https://doi.org/10.1016/j.csr.2008.03.003>, 2008.

Hilgen, F. J.: Extension of the astronomically calibrated (polarity) time scale to the Miocene/Pliocene boundary, *Earth and Planetary Science Letters*, 107, 349–368, [https://doi.org/10.1016/0012-821X\(91\)90082-S](https://doi.org/10.1016/0012-821X(91)90082-S), 1991.

Hilgen, F. J., Krijgsman, W., Langereis, C. G., Lourens, L. J., Santarelli, A., and Zachariasse, W. J.: Extending the astronomical (polarity) time scale into the Miocene, *Earth and Planetary Science Letters*, 136, 495–510, [https://doi.org/10.1016/0012-821X\(95\)00207-S](https://doi.org/10.1016/0012-821X(95)00207-S), 1995.

780 Jordà, G., Von Schuckmann, K., Josey, S. A., Caniaux, G., García-Lafuente, J., Sammartino, S., Özsoy, E., Polcher, J., Notarstefano, G., Poulain, P. M., Adloff, F., Salat, J., Naranjo, C., Schroeder, K., Chiggiato, J., Sannino, G., and Macías, D.: The Mediterranean Sea heat and mass budgets: Estimates, uncertainties and perspectives, *Progress in Oceanography*, 156, 174–208, <https://doi.org/10.1016/j.pocean.2017.07.001>, 2017.

Kemp, A. E., Pearce, R. B., Koizumi, I., Pike, J., and Rance, S. J.: The role of mat-forming diatoms in the formation of Mediterranean  
785 sapropels, *Nature*, 398, 57, 1999.

Krijgsman, W., Hilgen, F. J., Raffi, I., Sierro, F. J., and Wilson, D. S.: Chronology, causes and progression of the Messinian salinity crisis, *Nature*, 400, 652–655, <https://doi.org/10.1038/23231>, 1999.

Laskar, J.: Secular evolution of the solar system over 10 million years, *Astronomy and Astrophysics*, 198, 341–362, 1988.

790 Lourens, L. J., Antonarakou, A., Hilgen, F. J., Van Hoof, A. A., Vergnaud-Grazzini, C., and Zachariasse, W. J.: Evaluation of the Plio-  
Pleistocene astronomical timescale, *Paleoceanography*, 11, 391–413, <https://doi.org/10.1029/96PA01125>, 1996.

Malanotte-Rizzoli, P.: The northern adriatic sea as a prototype of convection and water mass formation on the continental shelf, *Elsevier Oceanography Series*, 57, 229–239, [https://doi.org/10.1016/S0422-9894\(08\)70070-9](https://doi.org/10.1016/S0422-9894(08)70070-9), 1991.

Marshall, J. and Schott, F.: Open-ocean convection: Observations, theory, and models, *Reviews of Geophysics*, 37, 1–64, <https://doi.org/10.1029/98RG02739>, 1999.

795 Marzocchi, A.: Modelling the impact of orbital forcing on late Miocene climate: implications for the Mediterranean Sea and the Messinian Salinity Crisis, Ph.D. thesis, University of Bristol, 2016.

Marzocchi, A., Lunt, D. J., Flecker, R., Bradshaw, C. D., Farnsworth, A., and Hilgen, F. J.: Orbital control on late Miocene climate and the North African monsoon: Insight from an ensemble of sub-precessional simulations, *Climate of the Past*, 11, 1271–1295, <https://doi.org/10.5194/cp-11-1271-2015>, 2015.

800 Matthiesen, S. and Haines, K.: A hydraulic box model study of the Mediterranean response to postglacial sea-level rise, *Paleoceanography*, 18, <https://doi.org/10.1029/2003PA000880>, 2003.

Meijer, P. T. and Dijkstra, H. a.: The response of Mediterranean thermohaline circulation to climate change: a minimal model, *Climate of the Past Discussions*, 5, 1731–1749, <https://doi.org/10.5194/cpd-5-1731-2009>, <http://www.clim-past-discuss.net/5/1731/2009/>, 2009.

Meijer, P. T. and Tuenter, E.: The effect of precession-induced changes in the Mediterranean freshwater budget on circulation at shallow and 805 intermediate depth, *Journal of Marine Systems*, 68, 349–365, <https://doi.org/10.1016/j.jmarsys.2007.01.006>, 2007.

Mikolajewicz, U.: Modeling mediterranean ocean climate of the last glacial maximum, *Climate of the Past*, 7, 161–180, <https://doi.org/10.5194/cp-7-161-2011>, 2011.

Myers, P. G.: Flux-forced simulations of the paleocirculation of the Mediterranean, *Paleoceanography*, 17, 9–1–9–7, <https://doi.org/10.1029/2000pa000613>, 2002.

810 Myers, P. G. and Rohling, E. J.: Modeling a 200-Yr interruption of the Holocene Sapropel S1, *Quaternary Research*, 53, 98–104, <https://doi.org/10.1006/qres.1999.2100>, 2000.

Myers, P. G., Haines, K., and Rohling, E. J.: Modeling the paleocirculation of the Mediterranean: The last glacial maximum and the Holocene with emphasis on the formation of sapropel S1, *Paleoceanography*, 13, 586–606, <https://doi.org/10.1029/98PA02736>, 1998.

on Oceanographic Tables, J. P.: Progress on oceanographic tables and standards, 1983–1986: work and recommendations of the Un- 815 esco/SCOR/ICES/IAPSO Joint Panel, no. 50 in UNESCO Tech. Pap. Mar., Unesco, 1986.

Pinardi, N., Zavatarelli, M., Adani, M., Coppini, G., Fratianni, C., Oddo, P., Simoncelli, S., Tonani, M., Lyubartsev, V., Dobricic, S., and Bonaduce, A.: Mediterranean Sea large-scale low-frequency ocean variability and water mass formation rates from 1987 to 2007: A retrospective analysis, *Progress in Oceanography*, 132, 318–332, <https://doi.org/10.1016/j.pocean.2013.11.003>, 2015.

Powley, H. R., Krom, M. D., and Van Cappellen, P.: Circulation and oxygen cycling in the Mediterranean Sea: Sensitivity to future climate 820 change, *Journal of Geophysical Research: Oceans*, 121, 8230–8247, 2016.

Raicich, F.: On the fresh water balance of the Adriatic Sea, *Journal of Marine Systems*, 9, 305–319, [https://doi.org/10.1016/S0924-7963\(96\)00042-5](https://doi.org/10.1016/S0924-7963(96)00042-5), 1996.

Roether, W., Manca, B. B., Klein, B., Bregant, D., Georgopoulos, D., Beitzel, V., Kovačević, V., and Luchetta, A.: Recent changes in eastern Mediterranean deep waters, *Science*, 271, 333–335, <https://doi.org/10.1126/science.271.5247.333>, 1996.

825 Rohling, E. J.: Review and new aspects concerning the formation of eastern Mediterranean sapropels, *Marine Geology*, 122, 1–28, [https://doi.org/10.1016/0025-3227\(94\)90202-X](https://doi.org/10.1016/0025-3227(94)90202-X), 1994.

Rohling, E. J. and Gieskes, W. W.: Late Quaternary changes in Mediterranean intermediate water density and formation rate, *Paleoceanography and Paleoclimatology*, 4, 531–545, 1989.

Rohling, E. J., Cane, T. R., Cooke, S., Sprovieri, M., Bouloubassi, I., Emeis, K. C., Schiebel, R., Kroon, D., Jorissen, F. J., Lorre, A., and Kemp, A. E.: African monsoon variability during the previous interglacial maximum, *Earth and Planetary Science Letters*, 202, 61–75, [https://doi.org/10.1016/S0012-821X\(02\)00775-6](https://doi.org/10.1016/S0012-821X(02)00775-6), 2002.

Rohling, E. J., Hopmans, E. C., and Damsté, J. S. S.: Water column dynamics during the last interglacial anoxic event in the Mediterranean (sapropel S5), *Paleoceanography*, 21, 1–8, <https://doi.org/10.1029/2005PA001237>, 2006.

Rohling, E. J., Marino, G., and Grant, K. M.: Mediterranean climate and oceanography, and the periodic development of anoxic events (sapropels), *Earth-Science Reviews*, 143, 62–97, <https://doi.org/10.1016/j.earscirev.2015.01.008>, <http://dx.doi.org/10.1016/j.earscirev.2015.01.008>, 2015.

Romanou, A., Tselioudis, G., Zerefos, C. S., Clayson, C. A., Curry, J. A., and Andersson, A.: Evaporation-precipitation variability over the mediterranean and the black seas from satellite and reanalysis estimates, *Journal of Climate*, 23, 5268–5287, <https://doi.org/10.1175/2010JCLI3525.1>, 2010.

Rossignol-Strick, M.: Mediterranean Quaternary sapropels, an immediate response of the African monsoon to variation of insolation, *Palaeogeography, Palaeoclimatology, Palaeoecology*, 49, 237–263, [https://doi.org/10.1016/0031-0182\(85\)90056-2](https://doi.org/10.1016/0031-0182(85)90056-2), 1985.

Santvoort, P., Lange, G., Langereis, C., Dekkers, M., and Paterne, M.: Geochemical and paleomagnetic evidence for the occurrence of “missing” sapropels in eastern Mediterranean sediments, *Paleoceanography and Paleoclimatology*, 12, 773–786, 1997.

Schroeder, K., Garcia-Lafuente, J., Josey, S. A., Artale, V., Nardelli, B. B., Carrillo, A., Gaćić, M., Gasparini, G. P., Herrmann, M., Lionello, P., Ludwig, W., Millot, C., Özsoy, E., Pisacane, G., Sánchez-Garrido, J. C., Sannino, G., Santoleri, R., Somot, S., Struglia, M., Stanev, E., Taupier-Letage, I., Tsimplis, M. N., Vargas-Yáñez, M., Zervakis, V., and Zodiatis, G.: Circulation of the mediterranean sea and its variability, *Elsevier*, <https://doi.org/10.1016/B978-0-12-416042-2.00003-3>, 2012.

Scrivner, A. E., Vance, D., and Rohling, E. J.: New neodymium isotope data quantify Nile involvement in Mediterranean anoxic episodes, *Geology*, 32, 565–568, <https://doi.org/10.1130/G20419.1>, 2004.

Slomp, C. P. and Van Cappellen, P.: The global marine phosphorus cycle: Sensitivity to oceanic circulation, *Biogeosciences*, 4, 155–171, <https://doi.org/10.5194/bg-4-155-2007>, 2007.

Slomp, C. P., Thomson, J., and de Lange, G. J.: Enhanced regeneration of phosphorus during formation of the most recent eastern Mediterranean sapropel (S1), *Geochimica et Cosmochimica Acta*, 66, 1171–1184, 2002.

Song, X. and Yu, L.: Air-sea heat flux climatologies in the Mediterranean Sea: Surface energy balance and its consistency with ocean heat storage, *Journal of Geophysical Research: Oceans*, 122, 4068–4087, <https://doi.org/doi:10.1002/2016JC012254>, 2017.

Soulet, G., Ménot, G., Bayon, G., Rostek, F., Ponzevera, E., Toucanne, S., Lericolais, G., and Bard, E.: Abrupt drainage cycles of the Fennoscandian Ice Sheet, *Proceedings of the National Academy of Sciences of the United States of America*, 110, 6682–6687, <https://doi.org/10.1073/pnas.1214676110>, 2013.

Stratford, K., Williams, R. G., and Myers, P. G.: Impact of the circulation on Sapropel Formation in the eastern Mediterranean, *Global Biogeochemical Cycles*, 14, 683–695, <https://doi.org/10.1029/1999GB001157>, <https://agupubs.onlinelibrary.wiley.com/doi/abs/10.1029/1999GB001157>, 2000.

Struglia, M. V., Mariotti, A., and Filograsso, A.: River discharge into the Mediterranean sea: Climatology and aspects of the observed variability, *Journal of Climate*, 17, 4740–4751, <https://doi.org/10.1175/JCLI-3225.1>, 2004.

Thomson, J., Mercone, D., De Lange, G. J., and Van Santvoort, P. J.: Review of recent advances in the interpretation of eastern Mediterranean  
865 sapropel S1 from geochemical evidence, *Marine Geology*, 153, 77–89, [https://doi.org/10.1016/S0025-3227\(98\)00089-9](https://doi.org/10.1016/S0025-3227(98)00089-9), 1999.

Topper, R. P. and Meijer, P. T.: The precessional phase lag of Messinian gypsum deposition in Mediterranean marginal basins, *Palaeogeography, Palaeoclimatology, Palaeoecology*, 417, 6–16, <https://doi.org/10.1016/j.palaeo.2014.10.025>, <http://dx.doi.org/10.1016/j.palaeo.2014.10.025>, 2015.

van Helmond, N. A., Hennekam, R., Donders, T. H., Bunnik, F. P., de Lange, G. J., Brinkhuis, H., and Sangiorgi, F.: Marine productivity  
870 leads organic matter preservation in sapropel S1: Palynological evidence from a core east of the Nile River outflow, *Quaternary Science  
Reviews*, 108, 130–138, <https://doi.org/10.1016/j.quascirev.2014.11.014>, <http://dx.doi.org/10.1016/j.quascirev.2014.11.014>, 2015.

Van Santvoort, P., De Lange, G., Thomson, J., Cussen, H., Wilson, T., Krom, M., and Ströhle, K.: Active post-depositional oxidation of the  
most recent sapropel (S1) in sediments of the eastern Mediterranean Sea, *Geochimica et Cosmochimica Acta*, 60, 4007–4024, 1996.

Wegwerth, A., Dellwig, O., Kaiser, J. Ô., Ménot, G., Bard, E., Shumilovskikh, L., Schnetger, B., Kleinhanns, I. C., Wille, M., and Arz,  
875 H. W.: Meltwater events and the Mediterranean reconnection at the Saalian-Eemian transition in the Black Sea, *Earth and Planetary  
Science Letters*, 404, 124–135, <https://doi.org/10.1016/j.epsl.2014.07.030>, <http://dx.doi.org/10.1016/j.epsl.2014.07.030>, 2014.

Weldeab, S., Emeis, K. C., Hemleben, C., Schmiedl, G., and Schulz, H.: Spatial productivity variations during formation of sapropels  
S5 and S6 in the Mediterranean Sea: Evidence from Ba contents, *Palaeogeography, Palaeoclimatology, Palaeoecology*, 191, 169–190,  
https://doi.org/10.1016/S0031-0182(02)00711-3, 2003.

880 Westerhold, T., Röhl, U., and Laskar, J.: Time scale controversy: Accurate orbital calibration of the early Paleogene, *Geochemistry, Geophys-  
ysics, Geosystems*, 13, 1–19, <https://doi.org/10.1029/2012GC004096>, 2012.

Westerhold, T., Röhl, U., Frederichs, T., Bohaty, S. M., and Zachos, J. C.: Astronomical calibration of the geological timescale: Closing the  
middle Eocene gap, *Climate of the Past*, 11, 1181–1195, <https://doi.org/10.5194/cp-11-1181-2015>, 2015.

Wu, P. and Haines, K.: Modeling the dispersal of Levantine Intermediate Water and its role in Mediterranean deep water formation, *Journal  
885 of Geophysical Research C: Oceans*, 101, 6591–6607, <https://doi.org/10.1029/95JC03555>, 1996.

Zervakis, V., Georgopoulos, D., Karageorgis, A. P., and Theocharis, A.: On the response of the Aegean Sea to climatic variability: A review,  
*International Journal of Climatology*, 24, 1845–1858, <https://doi.org/10.1002/joc.1108>, 2004.

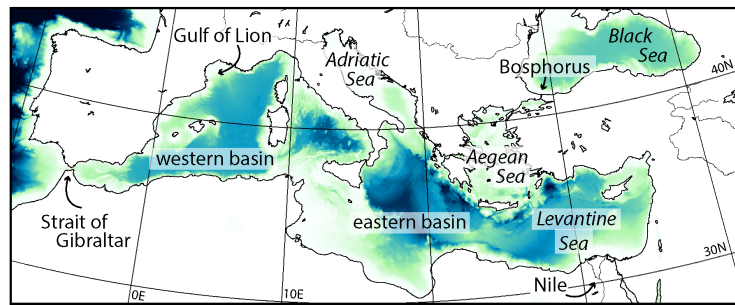


**Figure 1.** Map of the Mediterranean Sea. The bathymetry shown is part of the GEBCO 2014 Grid.

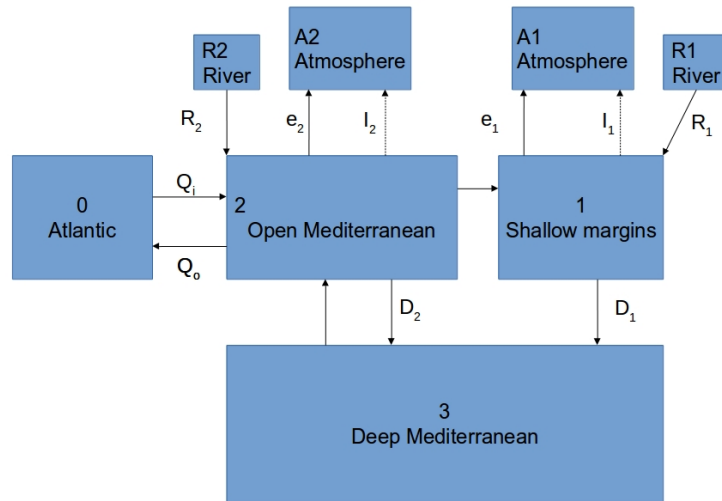


**Figure 2.** A schematic overview of the model set-up. The unlabelled fluxes are balancing fluxes, the equations for all fluxes are given in subsection 2.3. The direction of the arrows indicates the positive direction in the equations, all horizontal fluxes can change direction.

**Table 1.** All model parameters, excluding the model forcing.

Name	Value	Units	Description
$e_{\text{TA}} dt$	1.5	$\text{m}/\text{yr yr}$	Sea to air con-
$SFH c_A$	0.1	$\text{W}/\text{m}^2 \text{W}/(\text{m}^2 \text{K})$	Earth to sea he-
$c_{13}$	$1 \cdot 10^6$	$\text{s}^{-1} \text{kg}^{-1}$	Conductivity V
$c_{23}$	$4 \cdot 10^6$	$\text{s}^{-1} \text{kg}^{-1}$	Conductivity V
$c_{20}$	$3.9 \cdot 10^5$	$\text{m}^3/\text{s}/\sqrt{\text{kg}/\text{m}^3}$	Conductivity V
$k_{12}$	$1 \cdot 10^{-4}$	$\text{m}^2/\text{s}$	Hor. mixing be-
$L$	1000	$\text{m}$	Length scale o-
$k_{bg}$	$4 \cdot 10^{-5}$	$\text{m}^2/\text{s}$	background Ba-
$k_{str}$	$3.5 \cdot 10^{-4}$	$\text{m}^5/(\text{kg} \cdot \text{s})$	vertical Vertica-
$A$	$2.5 \cdot 10^{12}$	$\text{m}^2$	Surface area o-
$f$	0.2	—	Fraction of the
$d_1$	500	$\text{m}$	Depth of box 1
$d_2$	500	$\text{m}$	Depth of box 2
$d_3$	1000	$\text{m}$	Depth of box 3
$S_0$	36.2	$\text{kg}/\text{m}^3$	Salinity of the
$T_0$	15	$^{\circ}\text{C}$	Temperature o-
$T_{R1}$	16	$^{\circ}\text{C}$	Temperature o-
$T_{R2}$	18	$^{\circ}\text{C}$	Temperature o-
$\Theta + Q_1$	230	$\text{uM}$	Surface water
$\Theta e_B Q_{CO}$	$0.1 \cdot 1.1 \cdot 10^{-3}$	$\text{uM}/\text{yr} \text{s}^{-1}$	Biological oxy-
$\Theta e_A \cdot 0.1 \text{ } \mu\text{M}/\text{yr} \text{ Other oxygen consumption } - O_{CR}$	$0.1 \cdot 1.8 \cdot 10^{-7}$	$\text{uM} \cdot \text{s}/\text{m}^3 \text{m}^{-3}$	oxygen consum
$B_{th} c_p$	60 $\mu\text{M}$ Threshold $O_2$ concentration shr 4.187 $\cdot 10^3$	$\text{J}/(^{\circ}\text{K} \cdot \text{kg}) \text{ J}/(\text{K} \cdot \text{kg})$	Specific heat o-

**Table 2.** Forcing parameters that are the same for all runs

Parameter	Value	units
$R1\text{min}$	$5 \cdot 10^3$	$m^3/s$
$R2\text{min}$	$3 \cdot 10^3$	$m^3/s$
$e_{\text{max}}$	0.9	$m/yr$
TA1min	10	$^{\circ}C$
TA2min	12	$^{\circ}C$

**Table 3.** The variability of deep water oxygen over the interval where oxygen is below  $60 \mu M$  plotted against time step (each data point represents a model run) Forcing parameters that vary between runs.

Run name	R1max ( $m^3/s$ )	R2max ( $m^3/s$ )	emin ( $m/yr$ )	TA1max (deg $C$ )	TA2max (deg $C$ )
Reference run	$1.2 \cdot 10^4$	$3 \cdot 10^4$	0.75	10	12
Temperature variability run	$1.2 \cdot 10^4$	$3 \cdot 10^4$	0.75	13	15
fwb1 run	$1.2 \cdot 10^4$	$3 \cdot 10^4$	0.75	13	15
fwbtot run	$1.4 \cdot 10^4$	$8 \cdot 10^4$	0.74	13	15

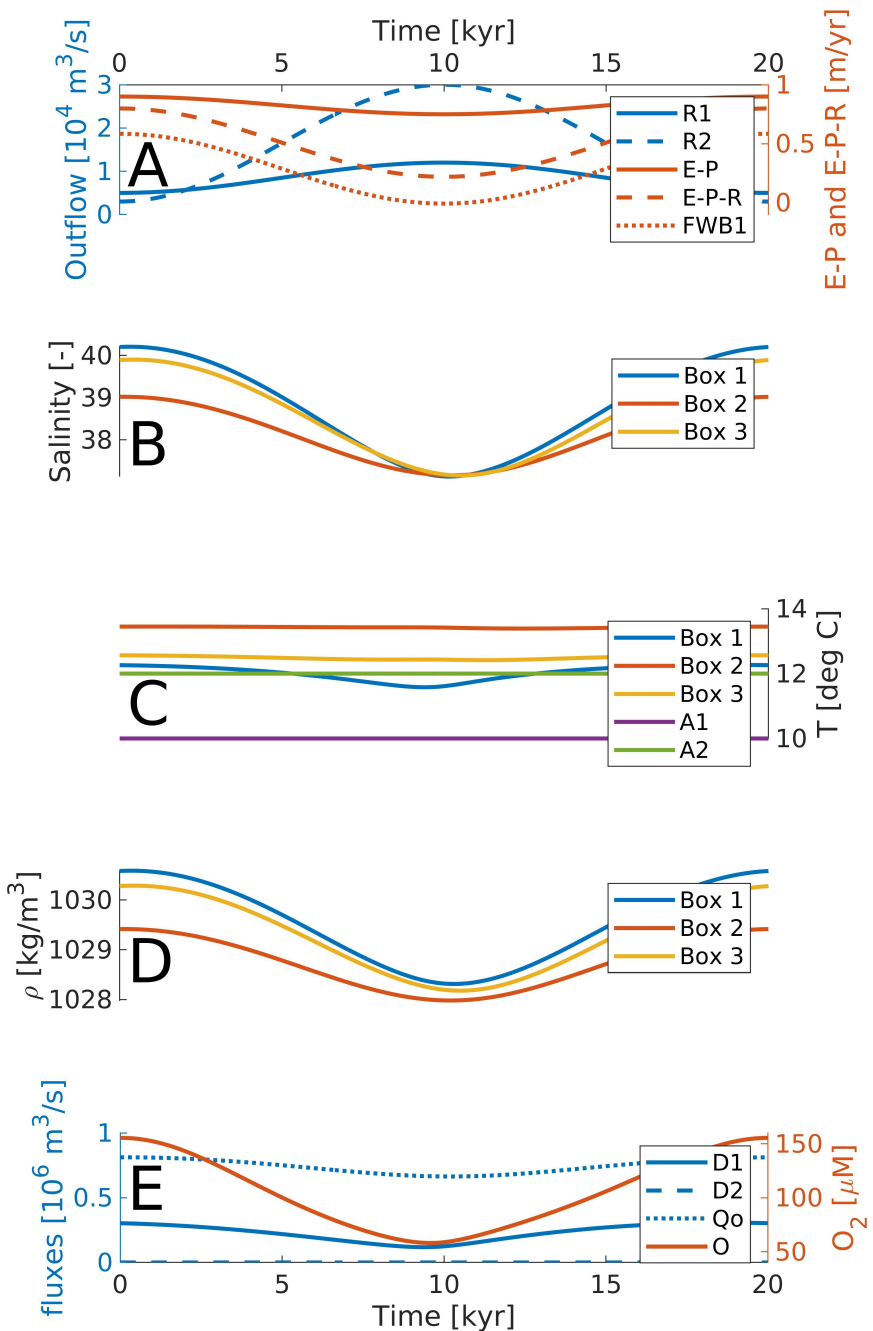


**Figure 3.** The forcing and results of the reference run. (A) The model forcing, with the river outflow on the left axis and the evaporation E-P, E-P-R and fresh water budget of box 1 on the right axis. (B)-(D) For each box respectively the salinity, temperatures, and densities. (E) The relevant fluxes (left axis) and the deep water oxygen concentration (right axis)

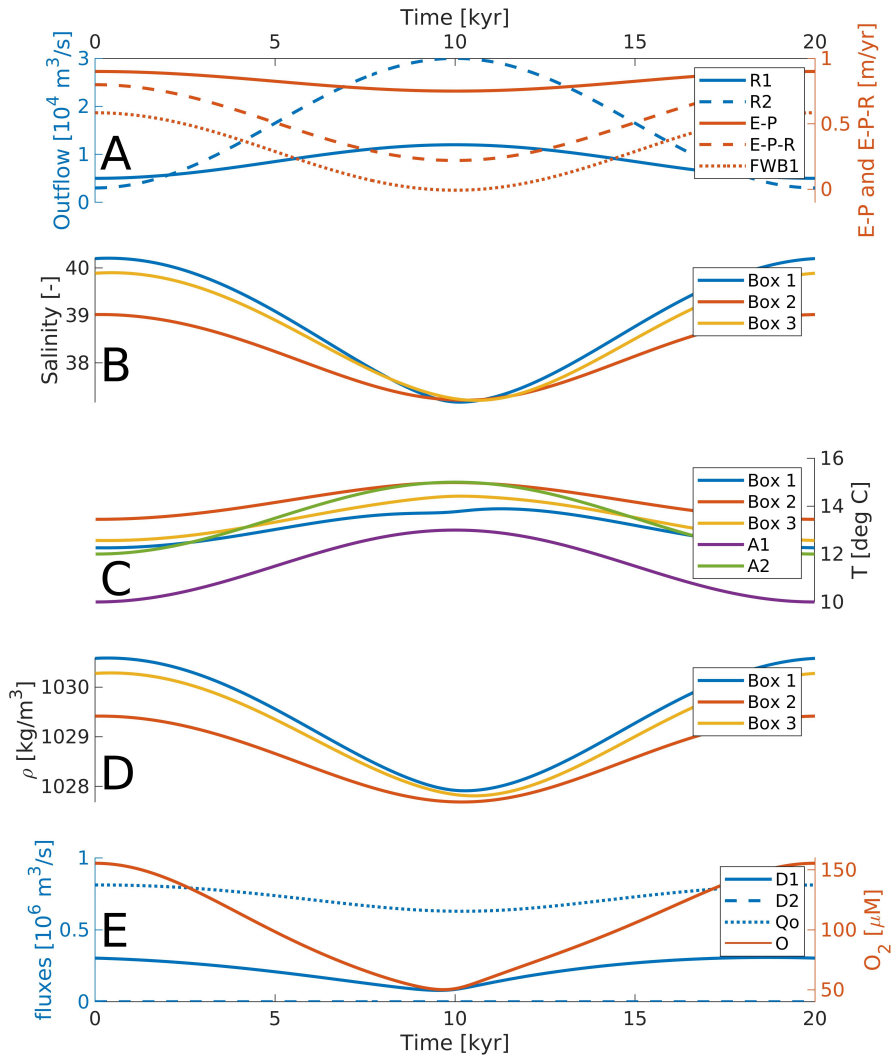


**Figure 4.** The forcing and results of the temperature-variability run. Layout of the panels is the same as in Fig. 3.

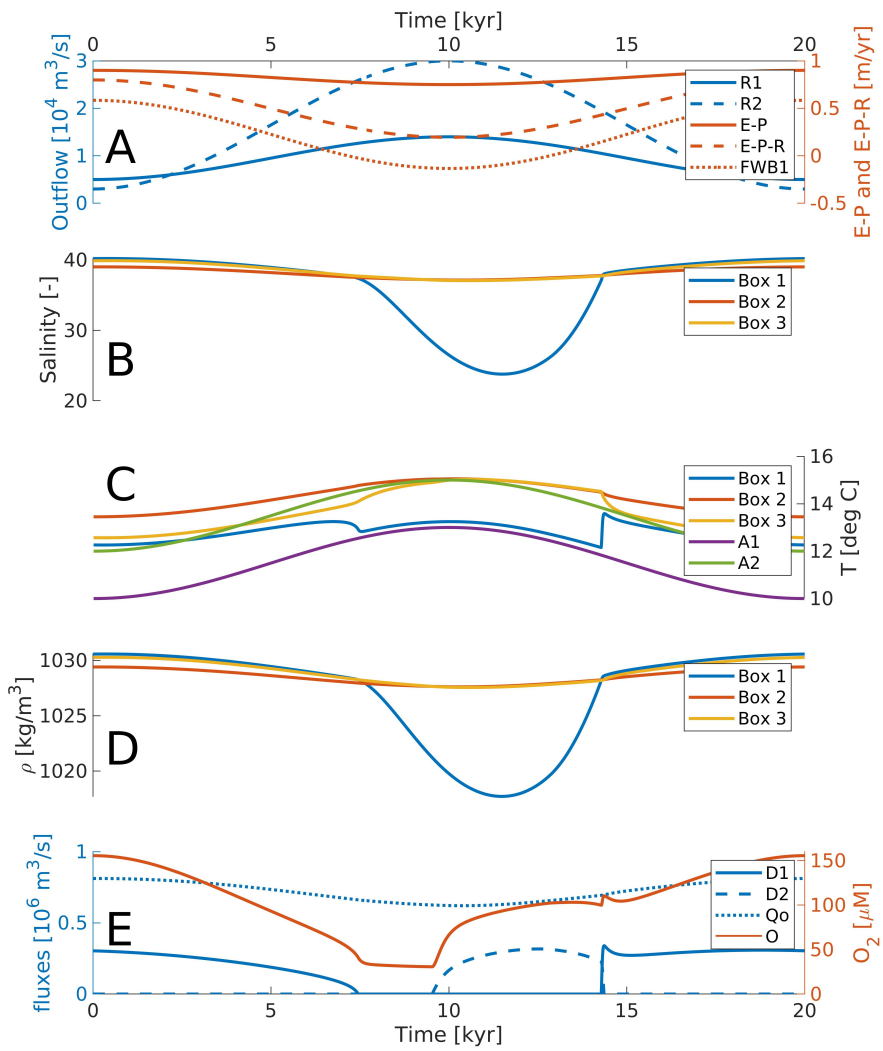


**Figure 5.** The forcing and results of the run where the freshwater budget of the margins becomes positive for a brief period. Layout of the panels is the same as in Fig. 3.

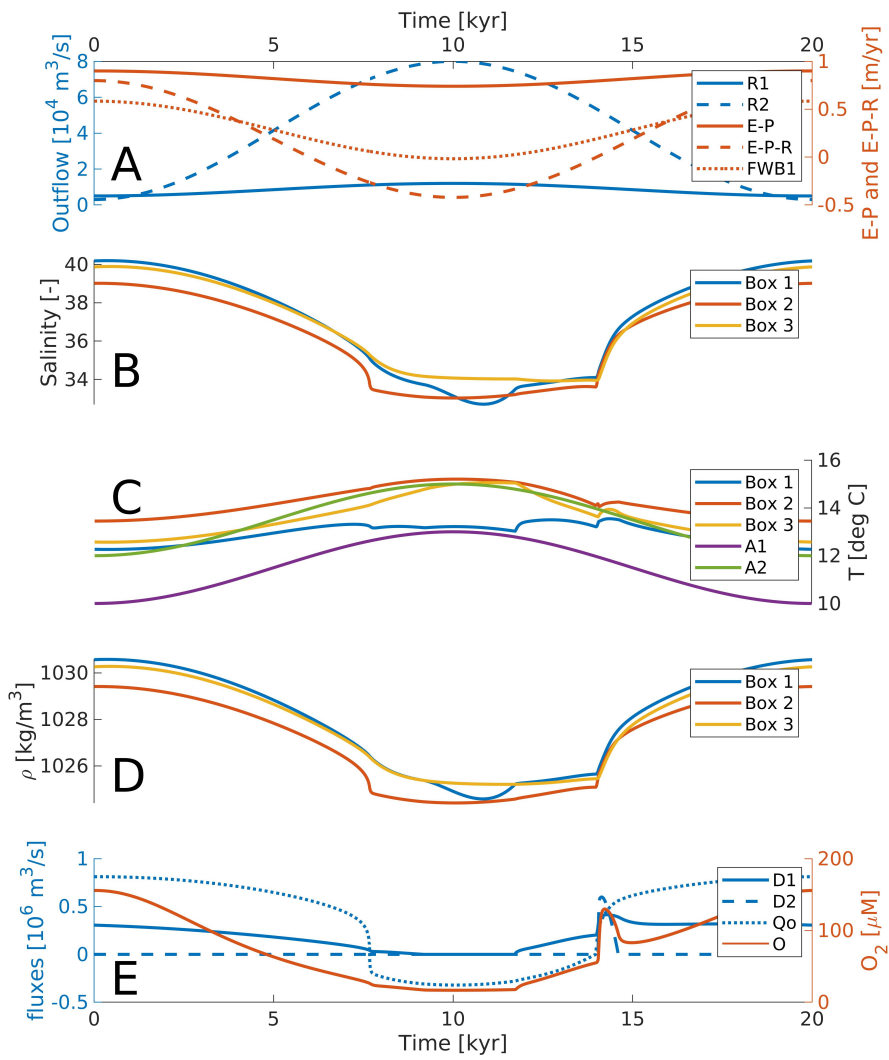


**Figure 6.** The forcing and results of the run where the freshwater budget of the whole basin becomes positive for a brief period. Layout of the panels is the same as in Fig. 3.

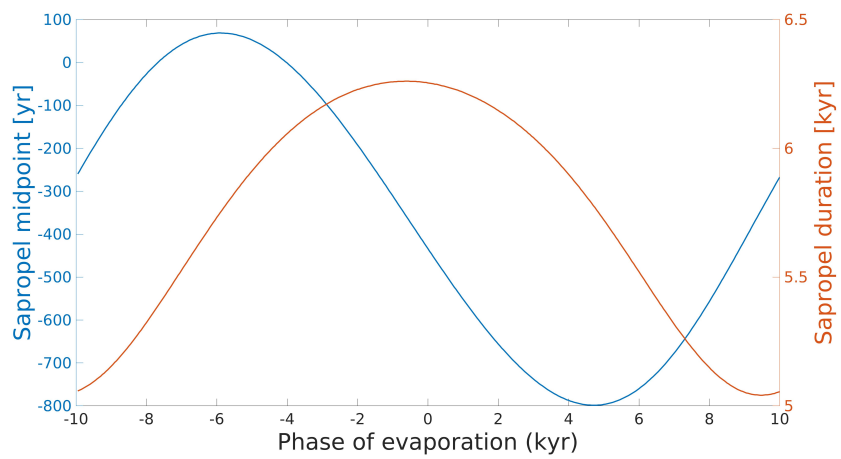


**Figure 7.** Sapropel duration (left-right axis) and timing of the midpoint relative to the precession minimum (on the right-left axis) as a function of the phase of evaporation. Apart from the phase of evaporation, the model forcing is the same as the [first run](#) in subsection [3.4.3.2](#).

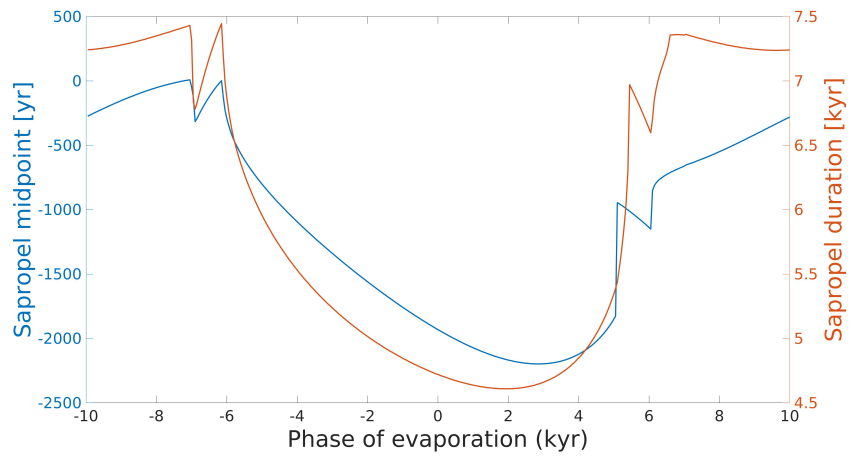


**Figure 8.** Sapropel duration (left-right axis) and timing of the midpoint relative to the precession minimum (on the right-left axis) as a function of the phase of evaporation. Apart from the phase of evaporation, the model forcing is the same as the first run in subsection 3.3